CHARACTERISATION OF BORON NITRIDE COATINGS

A MASTER'S THESIS

in

ManufacturingEngineering

Atılım University

by

TUĞÇE HACALOĞLU

JULY 2016

CHARACTERISATION OF BORON NITRIDE COATINGS

A THESIS SUBMITTED TO

THE GRADUATE SCHOOL OF NATURAL AND APPLIED SCIENCES

OF

ATILIM UNIVERSITY

BY

TUĞÇE HACALOĞLU

IN PARTIAL FULFILLMENT OF THE REQUIREMENTS FOR DEGREE OF

MASTER OF SCIENCE

IN

DEPARTMENT OF MANUFACTURING ENGINEERING

JULY2016

Approval of the graduate school of Natural and Applied Sciences, Atılım University.

Prof. Dr. İbrahim Akman

Director

I certify that this thesis satisfies all the requirements as a thesis for the degree of Master of Science.

Prof.Dr. EnginSadıkKılıç

Head of Department

This is to certify that we have read the thesis "CHARACTERISATION OF BORON NITRIDE COATINGS" submitted by "TuğçeHacaloğlu" and that in our opinion it is fully adequate, in scope and quality, as a thesis for the degree of Master of Science.

Prof. Dr. BilginKaftanoğlu

Supervisor

Examining Committee Members

Prof. Dr. BilginKaftanoğlu _____

Asst. Prof. Dr. ErkanKonca _____

Asst. Prof. Dr. SezerÖzerinç _____

(Date: 13.07.2016)

I declare and guarantee that all data, knowledge and information in this document has been obtained, processed and presented in accordance with academic rules and ethical conduct. Based on these rules and conduct, I have fully cited and referenced all material and results that are not original to this work.

Name, Last name: Tuğçe HACALOĞLU

Signature:

ABSTRACT

CHARACTERISATION OF BORON NITRIDE COATINGS

Hacaloğlu, Tuğçe

M.S., Manufacturing Engineering Department

Supervisor: Prof. Dr. BilginKaftanoğlu

July 2016, 94 pages

In this study, Boron Nitride (BN) coating is deposited by the magnetron sputtering - physical vapor deposition (PVD) technique.D2 steel substrates are coated with different allotropes of BNand are usedas substrates for characterisations. Single crystal grown hexagonal BN (h-BN) target is used and isconnected to a radio frequency power supply. Another powersupply connected to the substrate holder is used for substrate bias.Also, during this study the effects of the BN coating by using various coating parameters are investigated.

The thickness of the resulting coatings, friction coefficient, wear resistance are evaluated for mechanical properties and also nanohardness, and scratch behavior are measured. In addition, Fourier Transform Infrared Spectroscopy for crystal structure analysis (FTIR) technique is used for crystal structure of BN films.

The results of the investigations show that not only h-BN phases are obtained but also various different BN allotropes such as c-BN, w-BN, r-BN, t-BN, e-BN, a-BN are obtained.

Since there is more than one phase, surface properties are investigated for each case.Positive effects on the hardness and thickness are observed.Correlations between coating parameters and coating properties are discussed.

Keywords: Boron Nitride, Coating, Physical Vapor Deposition, BN allotropes, magnetron sputtering

ÖZ

BOR NİTRÜR KAPLAMALARIN KARAKTERİZASYONU

Hacaloğlu, Tuğçe

YüksekLisans, İmalatMühendisliğiBölümü

TezYöneticisi: Prof. Dr. BilginKaftanoğlu

Temmuz2016, 94sayfa

Bu çalışmada, Bor Nitrür kaplama (BN) Fiziksel Buhar Biriktirme yöntemi (FBB) - magnetron saçtırma tekniği ile biriktirilmiştir. D2 alttaş çeliği farklı BN alotropları ile kaplanmış karakterizsyonlarda kullanılmıştır. Radyo frekanslı bir güç kaynağına bağlı olan kristal büyütülmüş heksagonal Bor Nitrür (h-BN) hedef plakası kullanılmıştır. Diğer bir radyo frekanslı güç kaynağı alttaş tutucusuna bağlıdır. Karakterizasyonlar için alt taş olarak D2 çeliği kullanılmıştır. Ayrıca, farklı kaplama parametreleri kullanılarak BN kaplamadaki etkileri incelenmiştir.

Elde edilen kaplamaların kalınlık, sertlik, sürtünme katsayısı, aşınma direnci, yapışkanlık gibi mekanik özellikleri ve tribolojik ölçümleri için nano sertlik, tribometre, çizik testi cihazları kullanılarak değerlendirilmiştir. Ayrıca, kristal yapı incelemeleri için FourierTransform Kızılötesi Spektroskopisi (FTIR) tekniği kullanılmıştır.

Yapılan incelemeler sonucunda, h-BN fazı ile birlikte değişik allotropların da bulunduğu BN kaplamalar elde edilmiştir. Bu allotroplar; c-BN, w-BN, r-BN, t-BN, e-BN, a-BN dir.

Birden fazla fazın bulunmasından dolayı yüzey özellikleri çeşitli yönlerde etkilendiği gözlemlenmiştir. Sertliğe ve kalınlığa olumlu etkileri gözlemlenmiştir. Kaplama parametreleri ile kaplama özellikleri arasında elde edilen korelasyonlartartışılmıştır.

Anahtar Kelimeler: Bor Nitrür, Kaplama, Fiziksel Buhar Biriktirme Yöntemi, BN allotropları, Magnetron Saçtırma

To Mustafa Kemal Atatürk

ACKNOWLEDGMENTS

I would like to express my sincere gratitude to my supervisor Prof. Dr. BilginKaftanoğlu for his guidance, sharing, for his knowledge and understanding during this study. He encouraged me in each step from the beginning to the end of this study. I will be always grateful to him.

I would like to express my deepest thanks to NihanDökmetaş for her invaluable help and support during this studyand sharing her profound knowledge with me.

I would like to thank Alp Eren Sinan Özhan for his important support, advice and contributions to this research.

I would like to thank my colleagues EbruBallı and ArifeSağlam for their help and kind friendship. Especially, I thank to MerveGürbüz for her sincere friendship and help.

I would also like to thank Ms. İmren Yılmaz and the BEYÇELİK-GESTAMP Company for their joint project.

Thanks also go to Prof. Dr. NurdanÖzmeriçKurtuluş for the support provided by the TUBITAK project.

I would like to thank to my dear friends who were the witnesses of this stressful period and who alleviated this stressful load with their continuous encouragement and friendship.

I would like to thank to my mother NazanHacaloğlu, my father TuncayHacaloğlu, my sister Tuna Hacaloğlu, my uncle Mustafa Güney and my dear cousin Murat Güney for their indescribable love and endless support during my life.

TABLE OF CONTENTS

LIST OF FIGURES

FIGURES

LIST OF TABLES

TABLES

ACRONYMS

PVD – Physical Vapor Deposition

BN – Boron Nitride

h-BN – Hexagonal Boron Nitirde

FTIR – Fourier Transform InfraRed

c-BN – Cubic Boron Nitride

w-BN – Wurtizite Boron Nitride

r-BN – Rhombohedral Boron Nitride

t- BN – TurbsotraticBoron Nitride

e-BN – Explosive Boron Nitride

a-BN – Amorphous Boron Nitride

HSS – High Strength Steel

BK7 – Optical Glasses

B270- Optical Glasses

HRTEM – High Resolution Transmission Electron Microscopy

DC – Direct Current

RF – Radio Frequency

AFM – Atomic Force Microscopy

MST – Micro Scratch Test

SEM – Scanning Electron microscopy

NHT – Nano Hardness Test

ATR – Attenuated Total Reflectance

AE – Acoustic Emission

Pd – Penetration Depth

Rd – Residual Depth

TiN -Titanium Nitride

AlCrN- Aluminum Chromium Nitride

CrN – Chromium Nitride

AlTiN – Aluminum Titanium Nitride

CHAPTER 1

INTRODUCTION

In order to improve surface properties of a substrate, coatingsare used. Thick film coatings like galvanizing, chromium plating and plasma spraying are used against corrosion and wear. Thin film coatingsare employed to change the surface propertiesof metals and to extend the lifespan of certain mechanical parts such as tools, dies, molds, and some medical parts as seen in Figure 1.

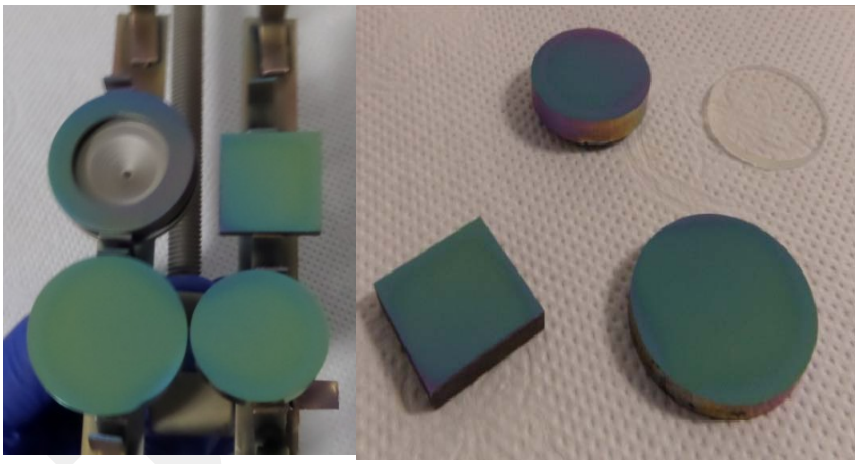

Figure 1. D2 steel, powder metallurgy steel, HSS and BK7 coated samples

Coating by electroplating uses acids which creates environmental problems and most of these processes are being converted to Physical Vapor Deposition (PVD). In industry, some companies use chromiumplating. Due to the environmental issue, such companies prefer PVD coating. PVD coating is an alternative to standard chromium plating method used to coat some vehicle rims. PVD is more environmentally friendly compared to traditional coating processes. Surface coatings have an extensive area of utilization in manufacturing industry. Shaping metals generates high temperatures and large mechanical forces resulting in high stresses at

the point of contact between workpiece and cutting/forming tools. Different solutions, like heat treatment and sintering, are developed to extend the tool life. Coating is one of these techniques.Modern technology requires thin films for the different cutting and forming applications not to change the tool and product dimensions, also to avoid the reduction of the sharpness of the cutting edges.The researchcarried out in physics and chemistry, resulted in the improvement of thin film studies applied in manufacturing industry.

Thickness of a thin film can range between tenths of a nanometer and several microns. Thin film coatings are important for the tool and die industry, in turn, influencing the manufacturing industry. Surface performance can be improved by covering it with a suitable coating.

In the PVD process, which is an atomistic deposition process, material is vaporized from target plate to substrate in the form of atoms or molecules and transported in the form of vapor through a vacuum. Coating processes are surface finishing processes.Low deposition temperature (200-500°C) makes the PVD process suitable for different types of steel grades.

PVD processes are realized in vacuum. Depending on the process used, the degree of vacuum required can be arranged. Degree of vacuum is a pressure in the vacuum chamber. Coating material and substrate (workpiece) materials are placed in a high vacuum chamber. Static or dynamic coating can be done by PVD technique. Operating parameters are determined according to the properties of the film. Film properties are measured by many techniques. Adhesion, thickness, nanohardness, atomic force microscopy (AFM), phase composition, tribologicaldata are measured. These kinds of measurements help the investigation of characteristic of boron nitride films. Boron nitride is preferred by virtue of several assets such as hardness of cubic structure, quality of transparency, using as a lubricant because of a hexagonal structure. BN films on different substrates may exhibit different properties. Good film quality depends on the related selection of the substrate and its surface condition. BN is a functional material and is very important in the structural sense.

Wear resistance of some tools and dies is generally a problem in industry. Due to this reason, the life of cutting tools and diesare limited. BNfilms improve the working life of cutting tools and dies.

In addition to these features, there area new properties of BN coatings for medical applications.For some medical applications like implants, it is important to have antibacterial, antifungal and osteoplastic properties. These properties are very important for implants and surgical instruments. BN coatings also show transparency in visible and infrared lightwhich makes it suitable as a coating material for optical lenses. With its high melting point (2950°C) it can be used for high temperature applications. Its protective ability against radiation is also well recognized.

Any metal can be coated on a base material through this process. In this thesis, Boron Nitride (BN) films are deposited on different substrates by a PVD- magnetron sputtering technique and characteristics are investigated.

CHAPTER 2

LITERATURE SURVEY

2.1. Definition of Boron and Boron Nitride

Boron (B) is a chemical element with an atomic number 5. Boron is also known as a metalloid [1]and is located between III and V group elements in the Periodic Table. Standard atomic weight is 10,811 g/mol. Elemental boron does not exist on earth.

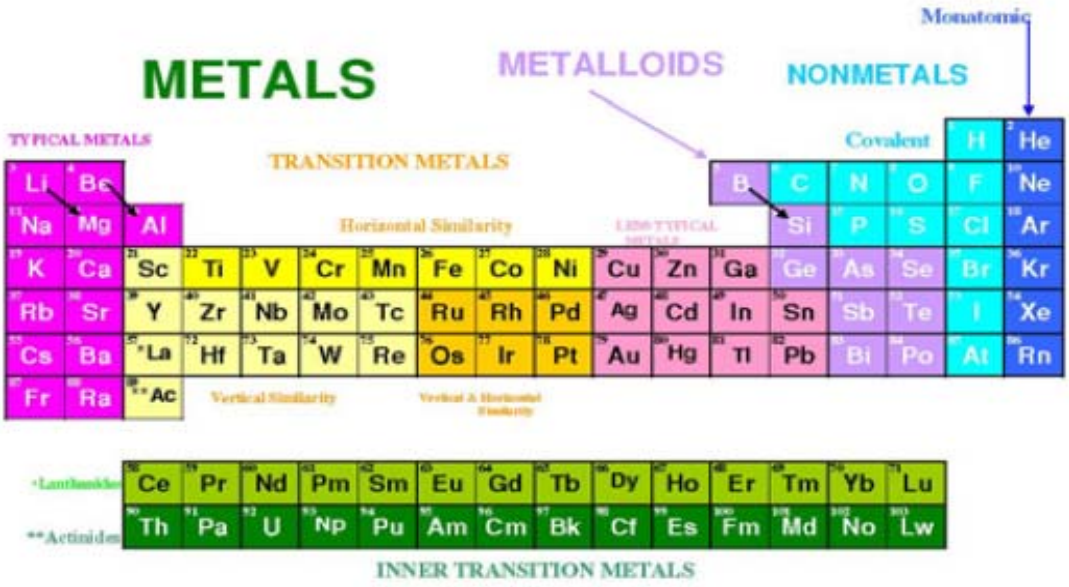

Figure 2. Periodic Table

Boron atoms have 5 electrons, 6 neutrons and 5protons. Its atomic diameter is 0.117 nm and its molar volume is 4,6cm^3/mol. In addition, crystal structure is a rhombohedral. Elastic modulus for bulk form is 320\GPa [2]. The ground state electronic configuration of natural Boron is $1s^2$ $2s^2 2sp^1$. Boron can form three

covalent bonds by sp^2 hybridization$1s^2\ 2s^1\ 2p_x^1\ 2p_y^1$, even though the boron atom in its normal electronic configuration has only one half filled orbital.

Figure 3. Boron

B10 and B11, both isotopes of Boron are used extensively in nuclear industry. B10 is used in the form of boric acid. Both isotopes can be used for the production of two radioisotopes: C11 and N13 [3]. Boron has isotopes ranging from B6 to B19, some of which have a very short life because of instability.The crystalline boron has four major allotropes: γ, β, α and T. β phase is known as a stable phase. On the other hand, other polymorphs are metastable at room temperature, transformation rate being negligible.

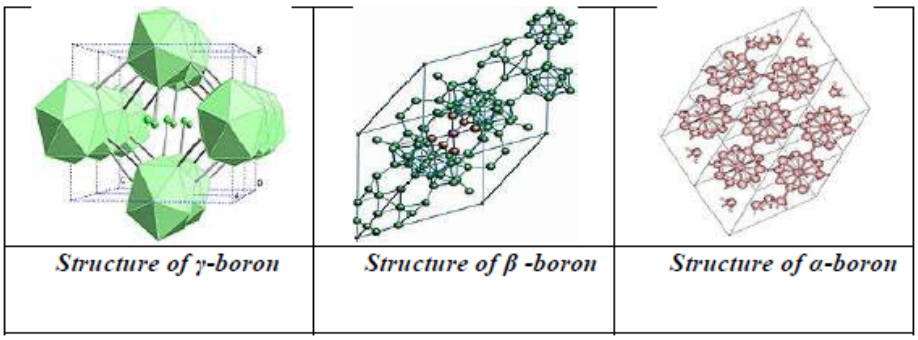

Figure 4. Structure of boron polymorphs

α -rhombohedral boron includes twelve atoms in a unit celland it is the most studied crystalline phase. T, tetragonal boron is another phase of boron. T-50 is known as a α- tetragonal boron and T-192 is known as a β-tetragonal boron. T-50 and T-192 phases contain 50 and 192 atoms per unit cell, respectively. γ- boron is producedby compressing other boron phases to 12-20 GPa with heating 1500- 1800°C. β- boron has a stablecrystal modification [4].

During this research, Boron Nitride (BN) films are produced and the different types of boron nitride allotropes (polymorphs) with their properties are characterized. The aim of the BN coating is to create new applications in industry. Boron nitride is a compound with the formula BN, consisting of equal of boron and nitrogen atoms. Metalor metalloids nitrides are prepared by giving a N_2 gas to vacuum chamber at high temperature. Boron,carbon and nitrogen are neighbor elements in periodic table. These elements are the basic components for super hard thin films.

Lie at al. reported that BN is easily produced from BCl_3(boron trichloride)and NH_3 (ammonia) through the following reaction: [5].

$$BCI_3 + NH_3 \rightarrow BN(s) + 3HC1 \qquad (1)$$

2.2. Allotropes of BN and Their Properties

Boron nitride crystallizes in at least four primary phases, hexagonal (h-BN), cubic (c-BN), wurtzite (w-BN), rhombohedral (r-BN) as shown in Figure 5. In addition to these four major phases, there are three more polymorphs. Explosive (e-BN), tetragonal (t-BN) and amorphous (a-BN).

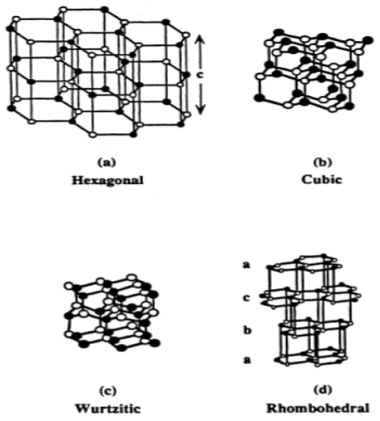

Figure 5. Crystal structure of boron nitride

Boron Nitride, BN, films have some important properties such as high stiffness, wear resistance etc. The surface of BN film is always covered with sp-bonded BN layers. Characterization of BN films requires the use of combination of several techniques. Crystal structure of BN has hexagonal rings made of three boron atoms and three nitrogen atoms, as shown in Figure 6.

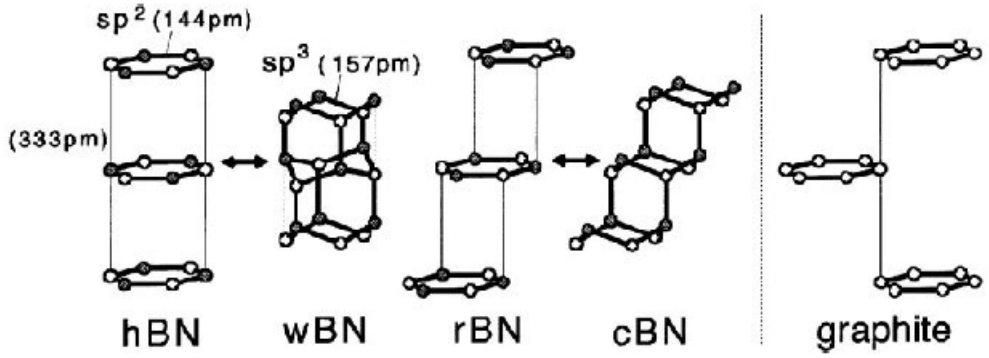

Figure 6. Structural relations of BN phases

h-BN and r-BN are sp^2 bonded. On the other hand, c-BN and w-BN are sp^3 bonded are shown in Figure 7 [6]. Each of which have similar characteristics to comparable

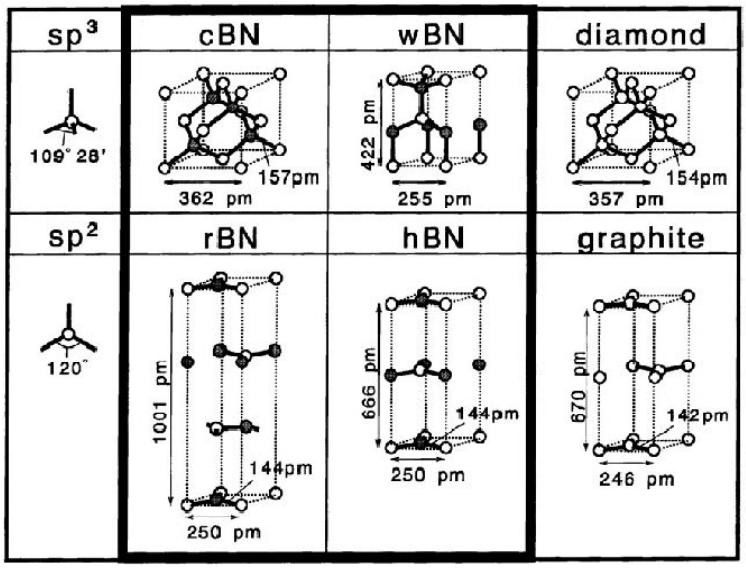

Figure 7. The four BN crystals

Two major forms of boron nitride are cubic (c-BN) and hexagonal (h-BN) boron nitride. These two allotropes have the same basic structure as the well-known carbon allotropes diamond and graphite. Mechanicalfeaturesof BN and C materials are similar. c-BN is known as super hard, almost as hard as diamond and h-BN is known as a soft and lubricious, like graphite [7]. c-BN thin films demonstrate excellent features including ultrahigh hardness, optical properties, high thermal conductivity [8]. Figure 8illustrates that the crystal structure of h-BN, along with the crystal structure of graphite as a comparison [9].

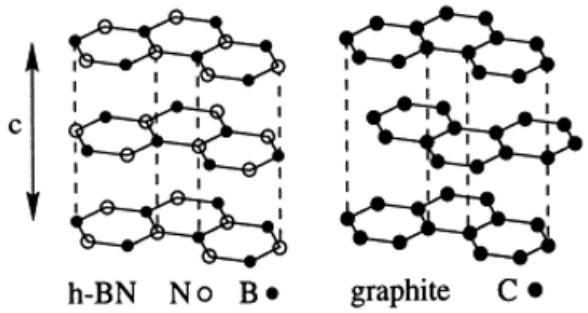

Figure 8. Structures of h-BN and graphite

h-BN was synthesized in 1842 by Balmain [10]. Boron nitride in the hexagonal modifications is an applicable insulating material for high temperature [11]. c-BN has a Vickershardness 45-55 GPa and secondin hardness only to diamond [10-12]. c-BN films have moreadvantages than diamond such as stability at high temperatures where diamond can burn over 400°C in the presence of oxygen. Structural data of BN allotropes are shown in Table 1 [8].

Table 1. Structural data of BN allotropes

	cBN	wBN	hBN	rBN
Lattice parameter a (Å)	3.6158	2.553	2.5044	2.504
Lattice parameter c (Å)	3.6158	4.22	6.66	1.001
Density (g cm^{-3})	3.49	3.45	2.34	2.2
Hardness (GPa)	40-60	/	10	/

For Boron Nitride as well as for Carbon a comparison can be made between the high density- high hardness allotropes, low density- low hardness allotropes. Crystallographic and chemical characteristics that are of interest for calculating the theoretical hardnessare illustratedin Table2 [12].Crystallographic characteristics for various boron nitride allotropes. The coordination number z, the lattice parameters a andc, the minimum interatomic spacing d (representing the length of the strongcovalent bond), the interlayer spacing d002, the roentgenographic density ρ are shown in Table 2[12].

Table 2. Crystallographic characteristics of Boron Nitride

Hybrid. state	Phase	Space group	z	a (A°)	c (A°)	d (A°)	d_{001} (A°)	ϱ (g/cm^3)	bond energy (eV)	
									cov.	van der Waals
sp^2	hBN	$P6_3/mmc$	3	2,504	6,661	1.4457	3.3306	2,29	3.25	0.052
sp^2	rBN	R3m	3	2,504	10,010	1.4500	3.34	2,29	3.25	0.052
sp^3	cBN	Fd3m	4	3,615		1.5670		3,51	1.52	
sp^3	wBN	$P6_3mc$	4	2,550	4,230	1.5760	2.20	3,50	1.52	-

Hexagonal boron nitride (hBN)isknown as a soft material and used as a lubricant[13].It has high electrical resistance, low dielectric constant and is chemically inert.

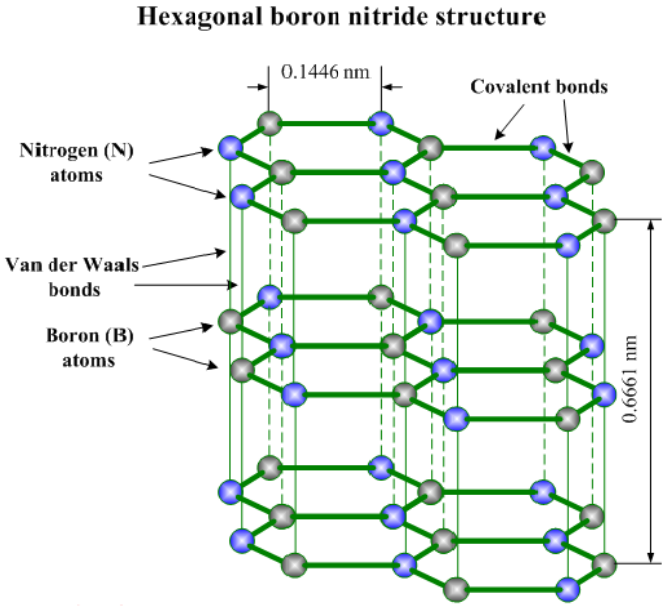

Figure 9.Hexagonal boron nitride structure

There is a covalent bond between Boron (B) and Nitrogen (N) atoms in the plane with an angle 120°. Furthermore, three boron atoms are bonded to three nitrogen atoms and each nitrogen atoms are bonded to three boron atoms.h-BN has largeapplication areassuch as:a) additive in lubricating oils, b) components of polymer based composite c) anti- friction material, d) solid lubricant in metal forming, e) sintered ceramic parts for high temperature applications [14]. h-BN is an electrical insulator and has a white color.Due to the lamellar structure of h-BN it is a natural lubricant.h-BN is also a good insulator with 5.2 eV direct gap value. [15].

Cubic boron nitride (c-BN) is known as a similar to diamond and was first synthesized by Wentorf in 1957 [16]. c-BN draws attention with properties as being the second hardest material to diamond, high thermal conductivity, has a wide band gap, E_g= 6.4 eV and hardness is 45-55 GPa. Elastic modulus is 850 GPa. On the other hand, c-BN does not react with ferrous materials. It is separated from the diamond with this feature [17]. Because of the hardness, c-BN is used as an abrasive and cutting tools material in sintered form [18]. These properties lead to a number of potential application in manufacturing industry. For tribological applications, c-BN film is selected as a protective coating such as in cutting tools [19]. The separation into layers by the addition of hydrogen gas has been reported [20].

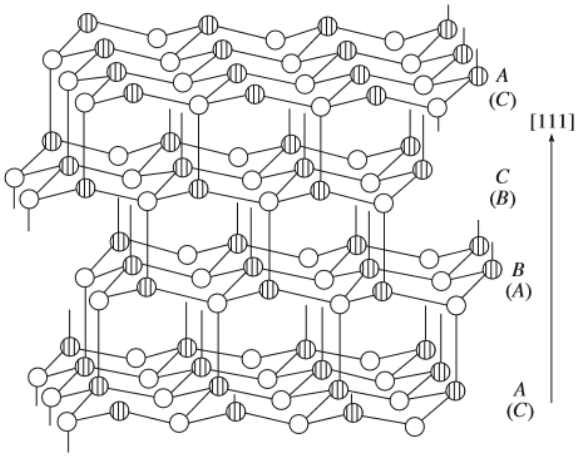

Figure 10. Structure of c-BN

c-BN has a very high thermal conductivity, good chemical inertness and excellent wear resistance. In addition to all these very useful properties, it has a high melting temperature (2973°C) [21]. c-BN is commonly used for cutting tools in manufacturing industry by virtue of its hardness. In recent investigations, some other properties of c-BN such antibacterial, antifungal and osteoblastic features have been found for use in the medical area. Theoretically at room temperature, the thermal conductivity of c-BN crystals is estimated to be 13W cm^{-1} K^{-1} [6]. A high strength and high thermal conductivity surfaces are widely demanded by many applications in industry. The oxidation temperature of c-BN is 1200°C which is way

higher than diamond (600°C). Density of c-BN is 3.48g/cm^3 [22]. Its thermal expansion value is 1.2x10^{-6} K^{-1}, compressive strength is 5,33 GPa [23]. Researchers reported that c-BN is a stable at high pressure- temperature conditions [24]. Physical properties of c-BN are as manifested given in Table 3 [25], [26].Some researchers reported that thickness of c-BN film can vary between 100 nm to 2 μm [27]. However, some film delaminations are observed due to residual stresses.

Table 3.Physical properties of c-BN

Properties	**c-BN**
Density (g/cm^3)	**3.48**
Thermal Conductivity, 25°C (W/m.K)	**1300**
Dielectric constant	**5.8**
Melting Temperature (°C)	**2973**
Oxidation Temperature (°C)	**1200**

Wurtzite boron nitride – (w-BN)is a phase of boron nitride and this phase is known as a highly defective metastable phase. According to chemical crystal characteristics w-BN and c-BN are metastable phases.

w-BN

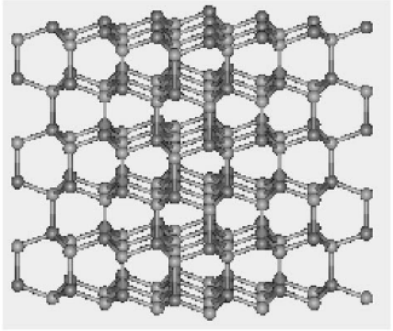

Figure 11. Structure of w-BN

Rhombohedral boron nitride – (r-BN) is rarely witnessed BN polymorphs. r-BN has also sp^2 bond structure as well as h-BN. Crystal structure of r-BN is given Figure 12. Along with the h-BN form, c-BN and w-BN structures of boron nitride was previously studied [28].

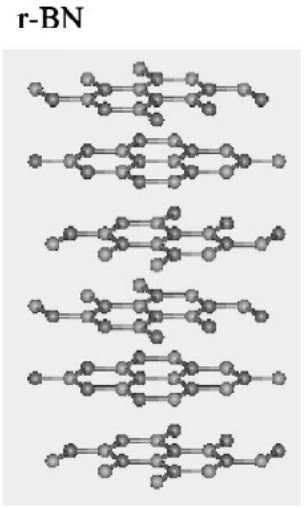

Figure 12. Structure of r-BN

Explosive boron nitride (e-BN) [29] was discovered by Batzanov et al. Subsequent to the studies conducted by Batzanov et al., e-BN was obtained by Akashi et al. The method used is explosive which is accomplished by a shock wave compression of h-BN powder [30]. Later, it was termed as explosive=e. e-BN has a face centered cubic (FCC) structure. There are no specific features. Today, researches about e-BN are still in progress. e-BN can be synthesized by vapor deposition method [31] [32]. e-BN is another allotrope of the BN and according to investigation of Lili et al. e-BN is converted into r-BN at 200-350°C. Furthermore, e-BN is converted into w-BN above 400°C and some of the w-BN is transformed into c-BN simultaneously.

Turbostratic boron nitride (t-BN)is anotherpolymorph of boron nitride. According to Petrescu et al. t-BN is a similar to h-BN but the order in c- axis direction is different [33].

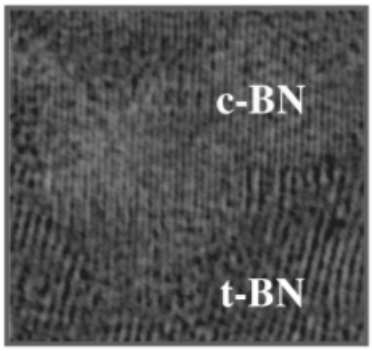

Figure 13. HRTEM images of the interface between t-BN and c-BN phase

Amorphous boron nitride(a-BN)According toMishima et al. [34] [35] there are two kinds of amorphous structures, t-BN and a-BN. t-BN has sp^2 structure and a-BN has sp^3 structure. One of them is similar to diamond-like- amorphous carbon and is called sp^3 –amorphous BN. Under low temperatures(about 600°C-800°C), boron formation is amorphous [36]. Some investigations proved that Stoichiometric thin films of a-BN are transparent and insulating [37]. According to Auger, a-BN films deposited by ion-beam-deposited and the band gap is about 5eV [38].

For boron nitride allotropes, pressure vs. temperature diagram is given in Figure 9 [39]. External factors, temperature and pressure, helps to make phase transformations between various BN amorphous.

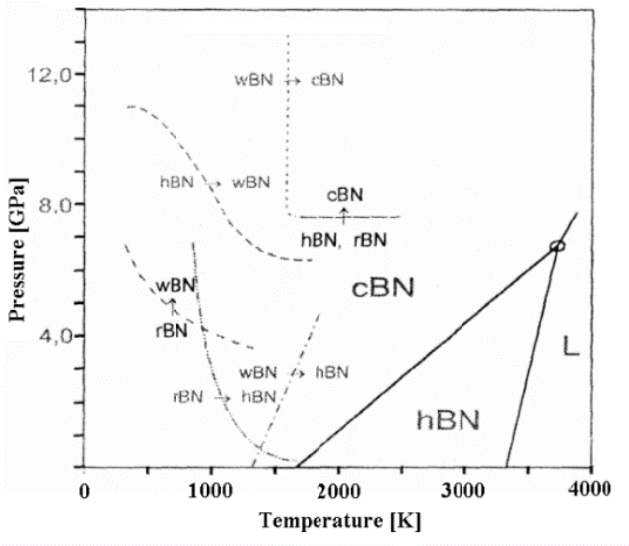

Figure 14. Phase equilibrium diagram of boron nitride polymorphs

According to researches, transformation of allotropes can be summarized as follows: *Lau et. al*states that experimental studies have shown that h-BN can be converted to w-BN by moderate heating. Depending on the lattice structures shown in Figure 15, conversion of h-BN, w-BN, r-BN and c-BN occurs. They hold the belief that there is a relation to small energy barriers. The energy barriers data calculated by Lau et. al [40].

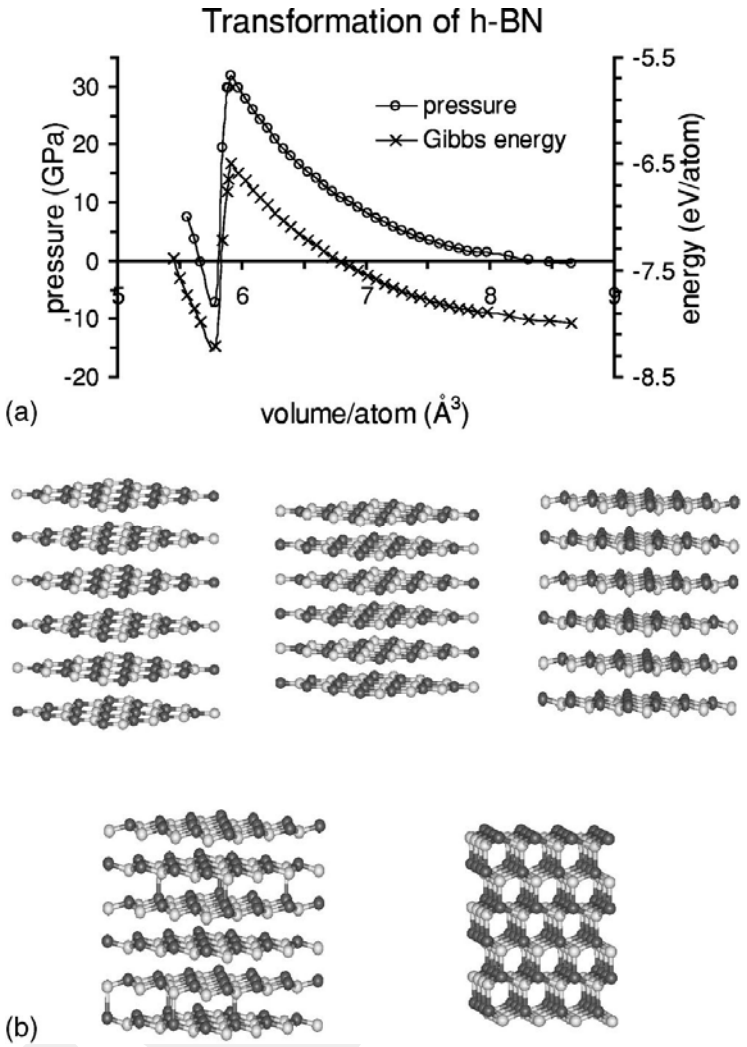

Figure 15. (a) Correlations among pressure, volume, and energy during transformation between h-BN and w-BN by compression. (b) Structural changes during transformation between h-BN and w-BN by compression.

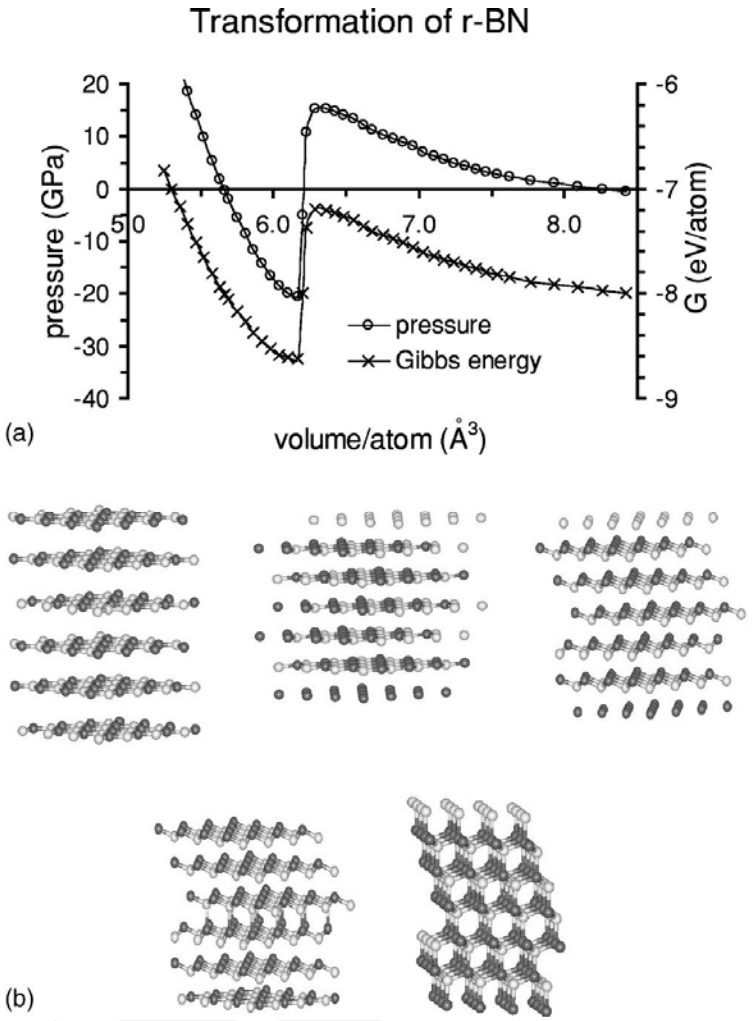

Figure 16. (a) Correlations among pressure, volume, and energy during transformation between r-BN and c-BN by compression. (b) Structural changes during transformation between r-BN and c-BN by compression.

Zhu et. al. reported that w-BN and c-BN have analogous properties. In addition to this, IR spectrum results with different deposition time are examined and states that when deposited time increases, main phase of film transformed from e-BN to w-BN. Zhu et al. states also one more important transformation about c-BN.

CHAPTER 3

SCOPE AND OBJECTIVE OF PRESENT INVESTIGATION

This study focuses on the characterization of the Boron Nitride (BN) coatingsdeposited on different substrates to be used in several applications. Previous investigations demonstrate that BN has a very large application area in industry and has the potential to play an important role in high tech industries.

The purpose of this study is to investigate the characterization of Boron Nitride coatings using experimental techniques. Many samples are coated using different coating parameters on different substrates. Each BN coating is tested for surface characterization and crystal structure.Correlations are attempted between the coating parameters and the characteristics of the BN film. This thesis first examines the preparation of the sample and deposition of the film, In the second stage, characterization of the thin film is investigated. Finally, the results of these characterizations are discussed with references to industrial applications.In every step, different parameters are investigated. In this manner, this systematic research will be an important contribution to possible optimization of the experimental parameters for the commercial production of boron nitride coatings.

CHAPTER 4

EXPERIMENTAL METHODS

4.1. Thin Film Deposition Process

Thin film means the deposition of a thin coatingto change the surface properties of a substrate for required applications. Surface modifications can be implemented by several processes. Among the many processes, coating techniques are used to modify the substrate surface properties. The main principle of the coating of a material is deposition of the film by atom by atom. Thickness of coating can range from several nanometers to several microns. This molecular deposition is performed in a vacuum, plasma, or electrolytic environment [41]. Vapor phase deposition of thin film layers can be implemented by various techniques [42]. In this research, BN film deposition is performed by physical vapor deposition (PVD). PVD is a method of coating that works under high vacuum. During the coating, material which is in the target plate evaporates in the vacuum chamber and intensifies onto the substrate surface. Most extensive PVD techniques are sputtering, thermal vaporization, arc vapor deposition and ion plating [43]. Sputtering is the most widely applied process to grow a thin filmby using a gas e.g. N_2, O_2 which react with the sputter material from a target. A schematic drawing of the simple sputtering process is shown in Figure 17[44].

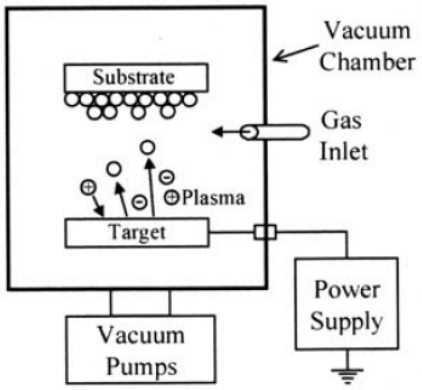

Figure 17. Schematic of a simple PVD sputtering system

4.2. BN Coating System

Bor-N coating system working at a high vacuum with double magnetron and target platesis used in this investigation. System provides a Direct Current (DC) and Radio frequency (RF) powered magnetrons for conductive and nonconductive target plates. (RF) voltage can also be applied to the substrate during deposition. This coating system shown in Figure 18 is manufactured by VAKSIS vacuum technology company in Ankara, Turkey.

Figure 18. PVD coating system

For BN film coating, a PVD type magnetron sputtering method is used. The vacuum chamber is controlled via the computer. There are additional system components such as heater, a cooling system for turbomolecular pump, etc. as seen in Figure 19.

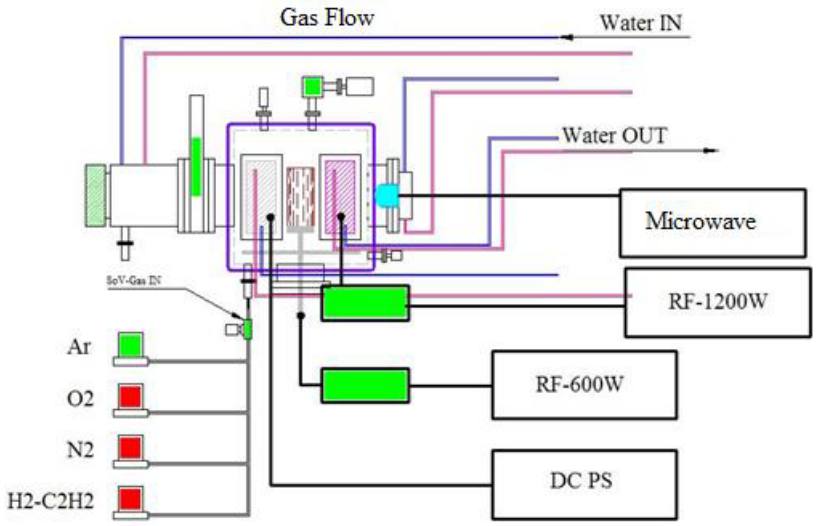

Figure 19. Schematic view of coating system

Unwanted gas molecules in the vacuum chamber are removed by heating the chamber by hot water and operating the mechanical vacuum pump.To obtain the desired vacuum, control panel is used as shown in Figure 20. Allcontrols are manually set. Various gases are used during the experiments. These gases are supplied to the vacuum chamber in order to generate plasma and perform coatings using the desired parameters. Argon (Ar) and Nitrogen (N_2), gases are used during the experiments. When the deposition is completed, dry nitrogen is used in orderto prevent coated samples from the oxidation and contamination.In the system, gas flow is controlled by a very sensitive valve. In BN coating laboratory gas tubes are located in a secure way. Flow rate is determined by control panel through manual settings. Chamber has four valves for four gases. Others are Hydrogen (H_2) and Oxygen (O_2). During this study, Ar and N_2gases are used. For future studies, other gases can be used. In the BN coating laboratory five gases are available. There is also an acetylene (C_2H_2) gas apart from the others. Italternately uses the same entrance with hydrogen.

Figure 20. Control panel

The process of film deposition occurs under high vacuum in a vacuum chamber. The vacuum chamber is a critical component of the system. The vacuum chamber walls are made of AISI 304stainless steel plates to resist high vacuum.

There are two magnetrons in the vacuum chamber. One is direct current (DC) magnetron, the other one is a radio frequency (RF) magnetron. Related target plates are inserted to these magnetrons. For metallic sputtering, DC magnetron is used such as for TiN coating.RF sputtering is performed atlow gas pressure (<1mTorr). For the low pressure plasmas, just as magnetron sputtering process, these particles involve electrons, neutrons, etc. that affect the surfaces. The effective temperature of the growing film rises due to the deposited energy [45]. In addition to these factors, the substrate material can be heated before and during the deposition with infrared radiation. Substrate materials can also be moved by planetary motion in order to ensure homogeneous coating. To obtain high vacuum, pumps are used. Mechanical pump is used for rough vacuum and turbo molecular pumpis used to get high vacuum.Coating can be applied while the substrate is static or making a planetary motion using the spindle. Mechanism of the spindle can be controlled manually and

is powered by an electric motor. During the experiments spindle speed is set to 30 rpm.

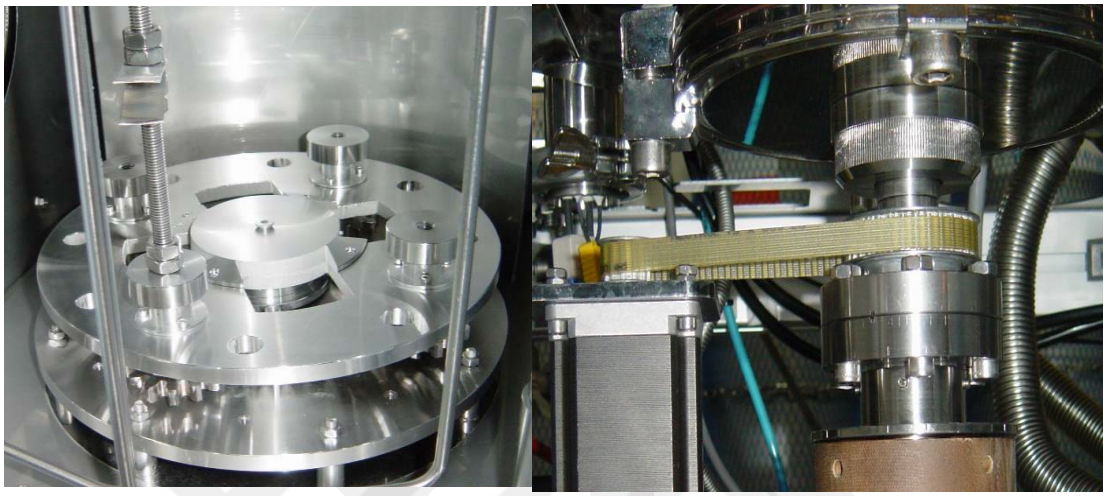

(a) (b)

Figure 21. (a)spindle and (b) motor mechanism

There are two heaters in the chamber. Two heaters are different from each other in the vacuum chamber. There is a thermocouple system in the heater. Heaters can keep the set temperatures of the chamber. Although the temperature limit of the system is 400°C, experiment temperaturesare set equal or below 300°C. Temperature control is performed by a PID method which is shown in Figure 22.

Figure 22. Temperature control device

Geometry of samples must be suitable for uniform coating. In addition to thetwo power supplies as mentioned above(RF, DC), microwave energy can also be used in

this system. RF and DC power supplies are used for sputtering deposition. Another RF system is directly connected to the spindle. This connection enablesthe plasma cleaning on substrates. Alternately, surface cleaning can be generated by microwave power supply. limit of substrate RF power supply is 600W, Limit of magnetron RF power supply is 1200W, limit of microwave power supply is 1400W and DC power supply rating is maximum 3000W. As a target plate, h-BN target plate is used. This plate is manufactured by the Materion Company and its dimension are 250x100x5 mm. It is mounted on a copper plate and is manufactured as a single crystal.

Figure 23. Single crystalh-BN target plate

High temperature and power can damage some of the components of the system. For this reason, a cooling system with a chiller is used to protect the pump and the system from overheating as seen in Figure 24.

Figure 24.Cooling system

Hot water circulation, provided by an electric water heater is used for degassing and initial heating of the system. Cold water provided by the chiller is used to cool the turbo molecular pump, magnetrons and the system.

Computer controls the PVD system. All process variables are controlled by the computer such as current, voltage and others. In addition to these main components, there are some subsidiary components such as compressor, air-conditioning system and uninterruptible power supply (UPS).

4.3. Procedure
4.3.1. Substrates

Several kinds of substrates are used for investigating the characterization of BN. In previous studies, AISI D2 steel is found to be a proper material to examine the characterization of BN. The scope of this thesis is characterization of BN coatings. Different substrates and their properties help the progress of this study. D2 steel is prepared according to the required size. Form has to be disc and having 30mm diameter with 5 mm thickness (Fig. 25and 26).

Figure 25. Ground sample

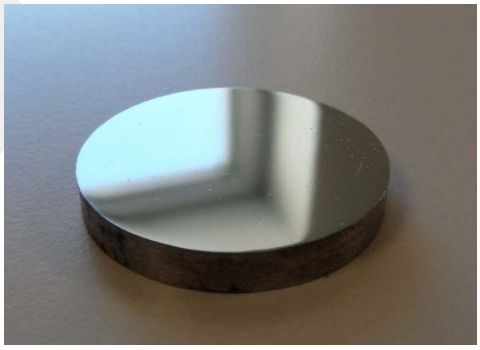

Figure 26. Polished sample

Additionally, optical glasses are used for characterization studies. Adhesion of BN coatings are examined on different materials such as Ti, high speed steel (HSS) AlTiN, TiN, TiAlSiN, TiAlN. In addition to all these different substrates some titanium implants are also coated.

4.3.2. Substrate preparation

4.3.2.1. Heat Treatment

Heat treatment is applied to increase the hardness of the D2 steel and it is an air hardening, high-carbon, high-chromium tool steel. Before applying a hard coating, the substrate should also be hardened so that it can withstand an indentation so that its deformation can be minimal. For this reason, samples of D2, are heated then they are quenched in order to increase their hardness. Heat treatment is applied to all AISI D2 steel samples using the facilities of the Metallurgical and Material Engineering Department of METU (Figure 27).

Figure 27. Heat treatment furnace

First, 30 mm diameter D2 steel rod is cut by a band saw in the Manufacturing Engineering laboratory ofAtılımUniversity to obtain samples with 6 mm thickness.Then, steel samples are heated up to 1040°C in the furnace (Figure 27) and then quenched rapidly in oil. Later they are tempered at 540°Cto get a hardness of around 54 HRC. In order to remove the oxide layer and toget a smooth surface, hardened steel samples are ground using a surface grinder.

4.3.2.2. Polishing

Preparation of the surface before the coating process is very important. After the initial grinding process, grinding continues with four kinds of sandpapers. These emery papers are 240, 400, 600 and 1000 grades. The sample is rotated 90° to obtain the desired surface of each grinding step to obtain a no directional surface. After the sanding process, polishing process starts. Samples are polished in two steps. 3µm and 1 µm polishing clothes are used with diamond suspension during this process. The prepared surfaces are checked under microscope in Figure 28.

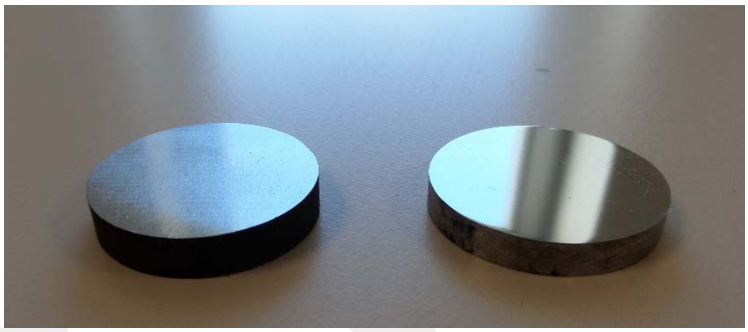

Figure 28. Ground and polished samples

4.3.2.3. Ultrasonic Cleaning

Before the coating process the prepared sample is required to have a very clean surface. Therefore, oxides and dirt on the surface are removed by ultrasonic cleaning. Cleaning system is shown in Figure 29.

Figure 29. Ultrasonic Cleaning System

Surface cleaning plays an important role in coating adhesion. Washing temperature is set to 52°C and duration is 15 minutes. After cleaning the samples, they are rinsed with water.

4.3.3. Holder Preparation for Substrate

Different kinds of substrates are coated during this study. Substrates have different shapes and dimensions. According to dimensions of vacuum chamber, holders are designed to keep the samples in proper position during the coating process as seen in Figure 30.

Figure 30.Samples of holders

4.3.4. System Cleaning

Contamination of the surfaces of the coating system is a serious problem since it causes electrical insulation and affects the adhesion property of the thin film. Therefore, it must be cleaned regularly to improve the functionality of the coating system. General maintenance and controls should also be made. The system iscleaned mainly by a sand blasting machine seen in Figure 31. Later it is wiped by alcohol and other solvents.

Figure 31.Sandblasting Machine

All sample preparation steps are illustrated in Figure 32 [46].

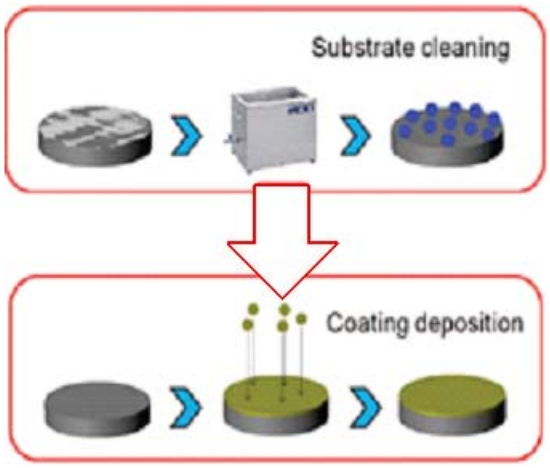

Figure 32. Phases of preparation

CHAPTER 5

CHARACTERIZATION FACILITIES

For the characterization of deposited thin film, F20 thickness measurements, micro/macro scratch test, nanoindentation test, atomic force microscopy (AFM), profilometer, tribometer, FTIR are used.

5.1. Thickness Measurements

There are various methods for measuring the thin film thickness. Since BN films are transparent in visible and infrared light, optical techniques can be used. Optical techniques arepreferred because they are non-destructive. F20 thin film analyzer is used to measure thickness and optical constants (Fig. 33). This instrument can measure thin-film characteristics by either reflecting or transmitting light through the sample. Also, the light over a range of wavelengths is analyzed with the same device.It can measure the thickness of the transparent film between 15 nanometers and 70 microns with a tolerance of ± 5 nm.

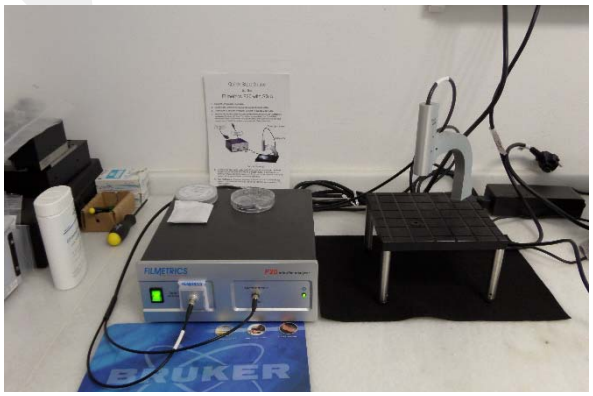

Figure 33. F20 thin film analyzer

5.2. Micro and Macro Scratch Test

The quality of adhesion of the thin film coating is characterized by both micro and macro scratch tests. In this test, the coated surface is scratched with diamond indenter. The load on the indenter can be constant or increasing with distance. During the test, sample moves at a constant speed [47].

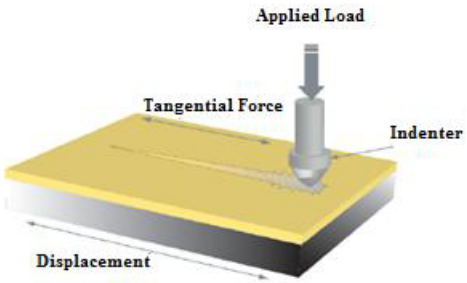

Figure 34. Scratch test

Scratch test is one of widely used, fast and effective methods obtain the critical loads (Lc) that are related to adhesion properties of coating. Each scratch is examined with an optical microscope for failure.

Figure 35. Macro Scratch Test Device

The load at which such failure of the coating occurs is termed as the critical load (Lc) [48]. Revetest® is a widely used test procedure for evaluation of coating(Fig.35). AFM figures of the scratch are as shown Figure 36.

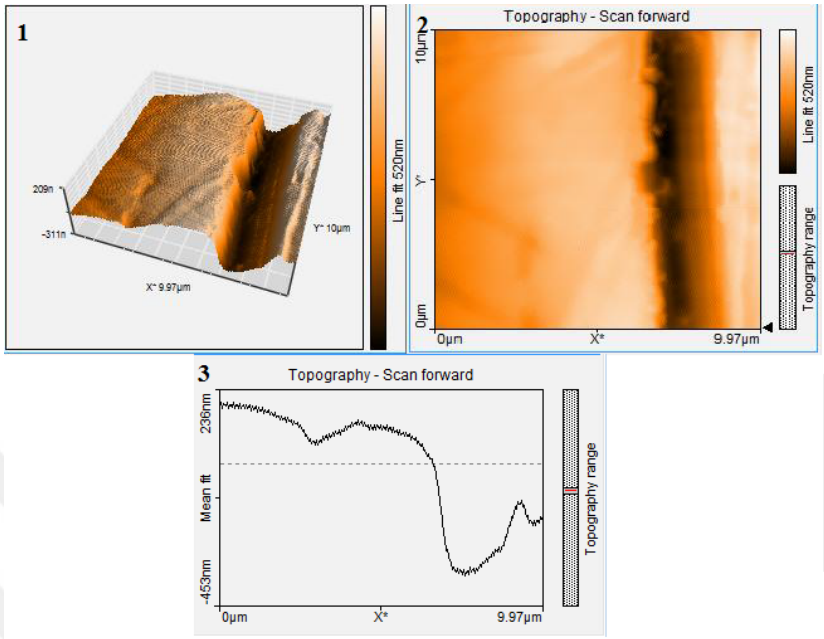

Figure 36.AFM images of Scratch with 3D (1), 2D topography scan (2), and 2D (3)

The Micro Scratch Tester® (MST) is used for the small specimens. Generally, MST is used to examine the coating thickness of below 5 µm. It is part of the open platform system which is shown in Figure 37.

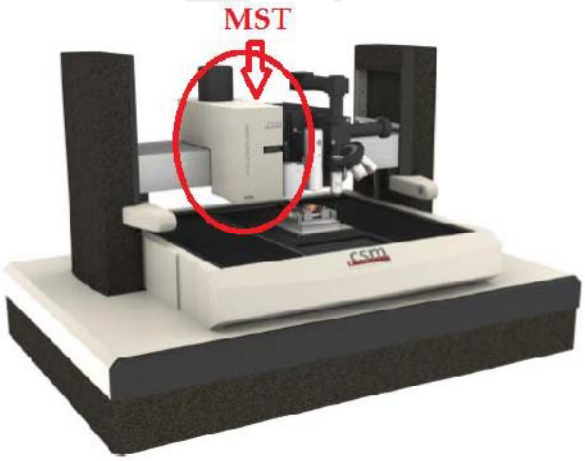

Figure 37. Micro Scratch Tester

Indenter type and the range of applied load are fundamental differences between these two devices. Both MST and Revetest® can be applied to different coated substrates such as metals, alloys, organic materials. Additionally, acoustic emission,

penetration depth and residual depth can be measured during scratch test. The scratch test parameters used in this thesis are given in Table 4.

Table 4.Properties of Micro\Macro Scratch Test

	Micro Scratch Test	**Macro Scratch Test/Revetest®**
Loading rate	59.94N/mm	299N/mm
Scratch Length	2mm	3mm
Indenter size-type	100µm Rockwell diamond indenter	200µm Rockwell diamond indenter
Indenter speed	4mm/min	6mm/min
Load (min.-max.)	0,03N-30N	0,5N-150N

this technique is a very old adhesion test method which developed from the scrape test. In the scratch test there is a stylus that is drawn over a film surface with constant or increasing load. The film may show deformations under the load. These deformations are examined under the microscope and critical loads are determined. Some measurements can be supported by scanning electron microscopy (SEM) images.

5.3. Nanohardness Test

Hardness measurement is often an important property of thin films especially for protective and tribological applications. Many important mechanical properties can easily be acquired by this test such as the Young's modulus andPoisson's ratio. During this study, coating hardness is measured with Nanoindentation test device which is shown in the Figure 38. Indentation tests are commonly used for testing the mechanical properties, especially hardness. Typically, a load is applied to material by an indenter, hardness value of the film is obtained by dividing the load by residual projected area of the indentation.

Figure 38. Nanohardness test device in open platform

The indenter depth penetration, h, and applied force, F, can be measured by NHT. Penetration depth and applied force are measured during load- unload cycle.

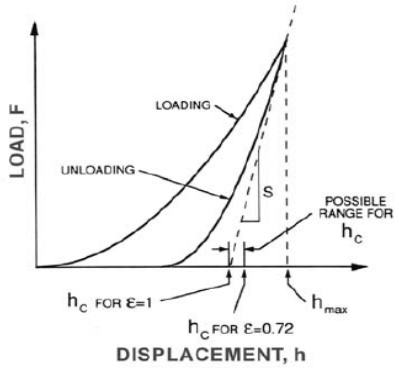

Figure 39. Typical representation of a load-displacement curve showing relevant quantities used in the analysis of hardness and elastic modulus [49]

Nanohardness test uses Oliver- Pharr method in order to calculate hardness and elastic modulus by using the measured force-displacement curve [50]. Oliver- Pharr method is the most common method for measuring the hardness and elastic modulus values. From force-displacement curve (Fig. 39),elastic modulus and hardness are calculated by this method. The hardness is normally calculated as;

$$H = F_{max} / A(h_c) \qquad (2)$$

where $F_{max}$is the maximum load and A(h_c)contact area at maximum load, calculated using the contact depth, h_c. $h_c$can be defined as at the vertical length along which the material fits the indenter.

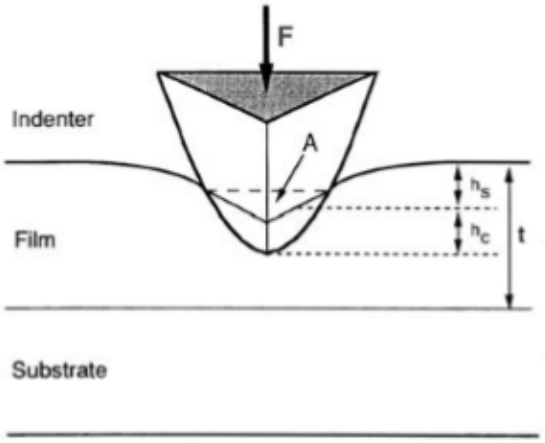

Figure 40.A schematic representation of an indentation showing relevant quantities used in the analysis of hardness *[50]*

Two apparent choices for the contact depth are the depth at peak load, h_{max} which is the maximum displacement in the loading cycle and the $h_f$which means residual depth of the impression after final unloading. At maximum load, the related maximum displacement h_{max} can be expressed,

$$h_{max} = h_c + h_s (3)$$

where h_s is the displacement of the surface at the primer of the contact. Based on the type of indenter used, h_s is given by,

$$h_s = \varepsilon F_{max} / S_{max} (4)$$

where ε is a geometric constant related to type of indenter and S_{max} is the initial unloading contact stiffness. The indentation hardness is finally obtained by combining three equations (2), (3) and (4).

Several loads are applied to determine the related loads to characterize the thin film. Film thickness has to be determined which is directly related with the penetration depth. That is taken as 10% of the film thickness in order to prevent the effect of the substrate. Berkovich type diamond indenter is used for measurements. Its diameter is 200 µm. 1mN and 5mN are applied to determined desired load depending on coating thickness for 10% penetration. Nanohardness mark can also be visualized by AFM as demonstrated in Figure41.

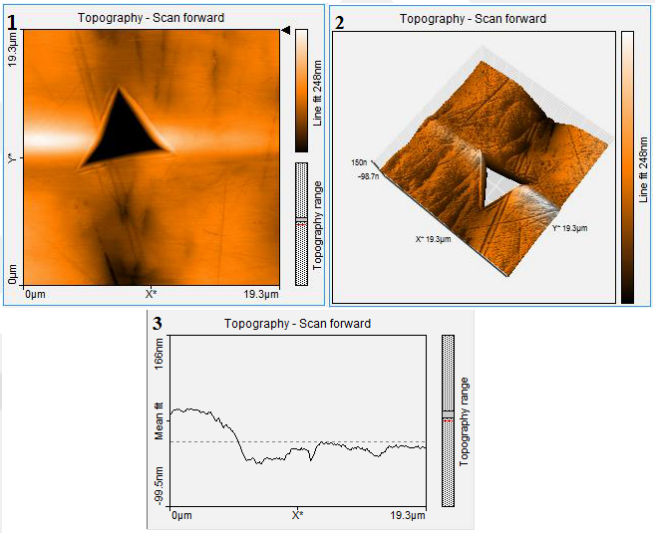

Figure 41.AFM images of NHT with 2D (1), AFM images with 3D (2) and AFM images with 2D Topography Scan (3)

5.4. Atomic Force Microscope (AFM)

AFM is a kind of scanning probe microscope (SPM). The surface roughness and topographic images can be measured by AFM (Fig. 42).

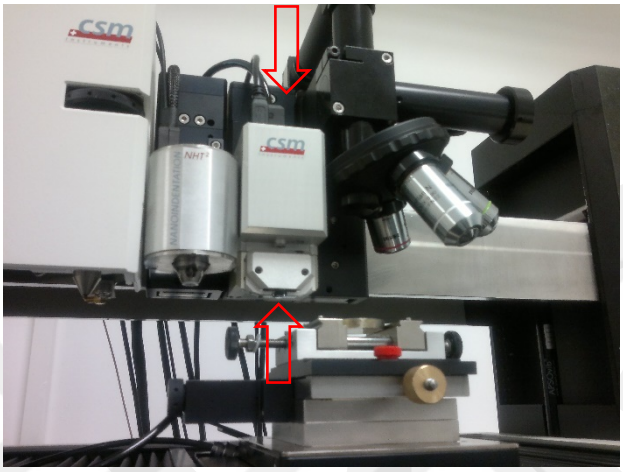

Figure 42. Atomic Force Microscope

Surface morphology of the thin film is examined by AFM [51]. The principle of atomic force microscope measurements is shown in Figure43. AFM provides a 3D profile of the surface in nanoscale by measuring forces and deflection between a sharp probe and surface for a very short distance.

The probe is generally supported on a cantilever. AFM tip slowly scans the surface and records the small force between the probe and surface. The probe generates the three dimensional displays with high resolution. In this research NanoSurf-Nanite-B version 2.2 CSM Instrument is used for topographic measurements. AFM tip does not damage the surface. Measuring parameters are as follows: The image size is 77x77 μm^2 area (Fig. 43), time/Line is 1s and points/line is 512.

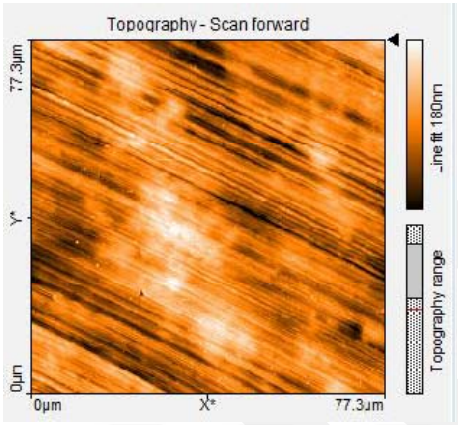

Figure 43. AFM images with 2D topography scan

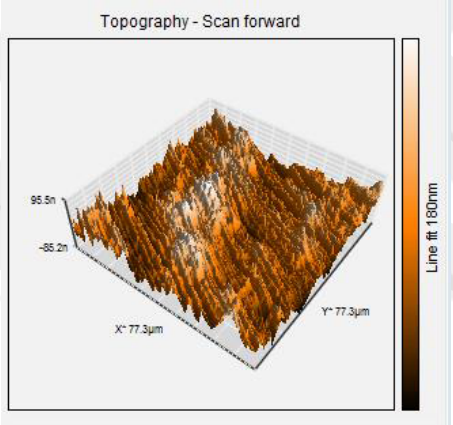

Figure 44. AFM images with 3D topography scan

5.5. Profilometer

Surface roughness is measured by Taylor Hobson Precision Surtronic 25 profilometerinstrument (Fig. 45) using Image Plus software. A diamond stylus is moved vertically on the surface of sample. The stylus moves laterally on the sample for a defined distance and defined contact force. Surface roughness is measured before and after the coatingdeposition in order to compare the results. Measurement parameters are as follows, Length of scrub is 4mm and range is 100 µm.

Figure 45. Taylor Hobson Precision Surtronic 25 profilometer

5.6. Tribometer Measurements

Friction coefficients and wear behavior of the film are examined using the standard tribometer. Aspherical or a flat probe is used with a certain weight during the test. Rotating or reciprocating linear motion is used. Friction coefficient of BN films are measured by the tribometer test. Tribometer is a device (Fig. 46) which measures the traction force of the contact and the normal force quantities and calculates the coefficient of friction between the two surfaces and plots it as a function of time. The sliding friction test takes place between a stationary pin stylus which is steel/alumina ball and a rotating disk having the sample material. Normal load, rotational speed, and wear track diameter can be determined. Tests are performed without lubricant. Friction force is measured during test with a load cell. For each test, ball surface is changed tohave a new surface is contact with the disc. Friction coefficient is calculated from the equation 5:

$$\mu = F_f / F_n \quad (5)$$

Where F_f is measured tractive friction force, F_n applied normal force[52].

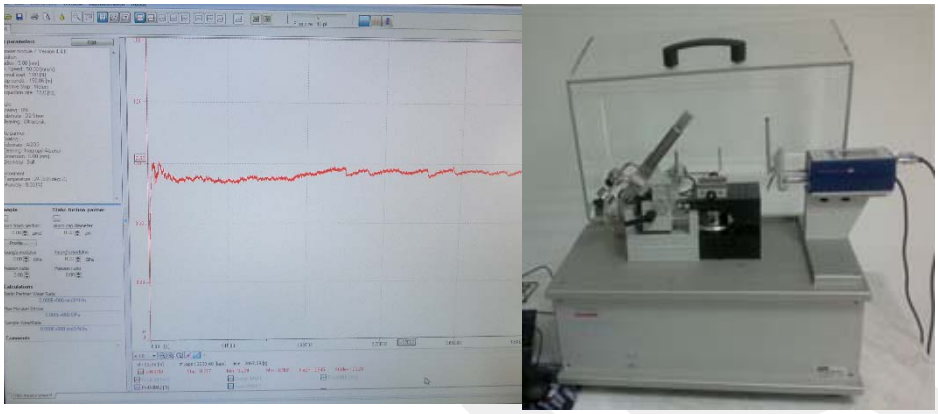

Figure 46.Tribometer and Profilometer test devices

5.7. Fourier Transform Infrared Spectroscopy (FTIR)

FTIR measurements are used to examine the characterization of coated samples which is shown in Figure 47. IR spectroscopy is based on the infrared light mainly absorbed by the examined substance. Absorption, the necessary amount of wave energy to bond the vibration and rotation of molecules is being sent from the infrared region of the electromagnetic spectrum by the device. FTIR is a non-destructive technique for solid and thin films used for quantitative analyses. In this study, BRUKER FTIR in Attenuated Total Reflection (ATR) mode with OPUS software is used to obtain infrared spectra in absorbance versus wavelength.

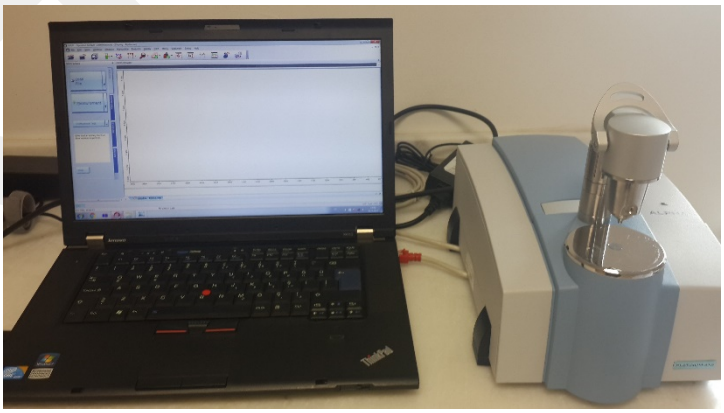

Figure 47. FTIR

CHAPTER 6

RESULTS AND DISCUSSION

6.1. Thickness Measurements

Thickness measurements are performed by Filmmetics® F20 thin film analyzer which can measure from 15nm to 70microns.BN films are measured by F20 because BN coatings are transparent in the visible and infrared lights. BN film thicknesses are measured approximately as 20nm-4000nm. The thickness value of the film changes depending on the substrate voltage. There are many different coating parameters: one of them is Substrate voltage = 250V.

When the substrate bias voltage is 250 volts during 6 hours in experiments, the thickness is in the 20-100 nm range.

The other type of coating parameter is one-hour coating with 100V and remaining 5 hours without substrate voltage.Without using spindle mechanism during 6 hours, 1 hour is 100V applied and remaining 5 hours are without substrate voltage. 100 volts for one hour contributes to thegrowth of a thicker thin film. In such experiments, coating thickness is between 500nmand 4μm.It is the different parameter than the others because it has multi- layered coating in itself.

In some experiments, microwave power is used. It is used as an additional power to magnetron and substrate power.Some experiments in which microwave power is used and the coating thickness is approximately 1μm.

Investigations of thickness measurements show that the substrate voltage significantly affects of thickness. Increaseof the substrate bias voltage decreases the thickness of the coated film. One-hour coating with 100V + 5 hours without substrate

voltage provides the thickest film around 4 μm. All thickness results are given in Appendix IV.

6.2. Adhesion Test Results

Adhesion is defined as twosurfaces held together by interfacial forces. These forces can be chemical bonds or VanderWaals forces. The scratch test is performed by applying a linearly increasing load on the coating surface. Some loads are defined as a critical load (L_c) which gives an information about the adhesion of the film. There are many techniques to determine the critical load. The critical loads and the adhesion quality can be determined with microscopeimage observations. In addition, some substrates have a failure due to their structure.The details of applied parameters are given in Table5.

Table 5.Scratch Test Measurement Parameters

Indenter type	Rockwell diamond type
Load Range	0.5N,1N-150N
Indenter radius	200μm
Scratch length	3mm
Load type	Linearly increasing

Coated steel samples are used for scratch test.Acoustic emission (AE), penetration depth (Pd), residual depth (Rd), friction coefficient (μm) are calculated during the test. For evaluating the measurements, last point of scratch is used.

According to scratch test results, RUN58 demonstrates that its adhesion is high because thescratch started after 57N in Figure 48. Also, RUN58 contains the highest percentage of c-BN.On the other hand, RUN122-1 has a maximum adhesion because scratch started in 59N which is demonstrated in Figure 49.The coating parameter is different and it is the one that has the highest adhesion. RUN91 is another sample which has high adhesion. Experiments performed at maximum power in RUN91 (Fig. 50).

Some samples are not uniform that means adhesion is not good. It can be seen in figure 51. Cracks occurs in RUN62, RUN79 samples (Fig. 54) Different type of substrate voltage is applied. Results show that substrate voltage is important.All measurements results are given in Appendix V.In addition to this, Adhesion measurements of the BN coating and TiN coating are investigated in Figure 52. The results demonstrate that cracks occur on TiN coating even when the same parameters for BN are applied. The thickness of TiN coated sample is 2µm and BN coated sample thickness is 1µm. Nevertheless, cracks of TiN coated samples demonstrate that adhesion of BN coating is better than that of TiN coating.

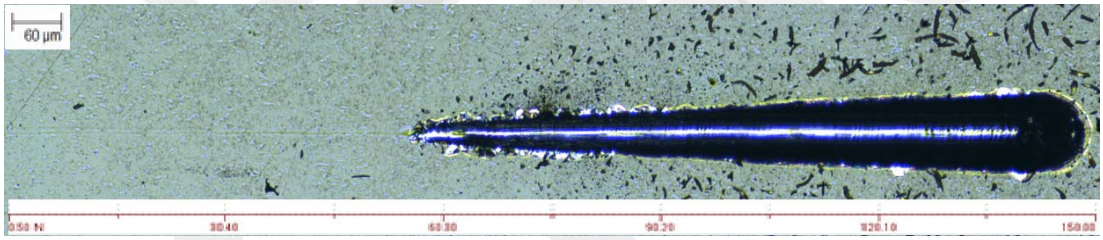

Figure 48. Scratch Test of RUN58

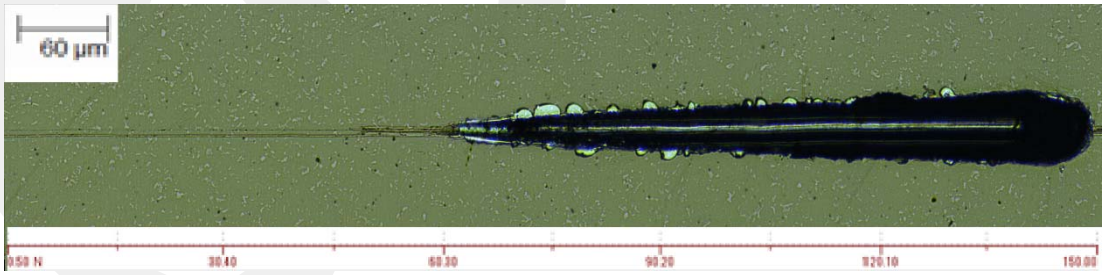

Figure 49.Scratch Test of RUN122-1

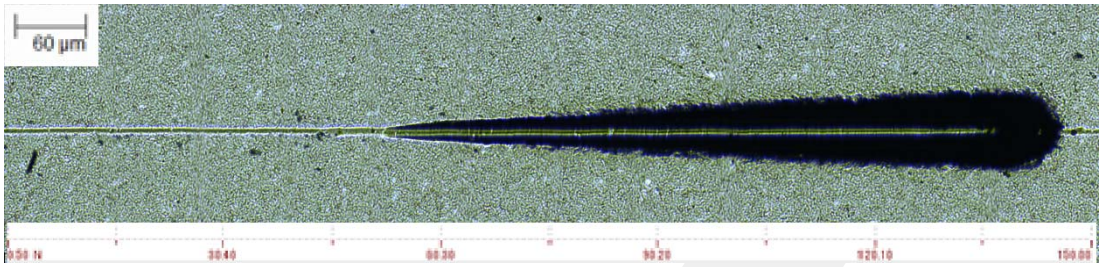

Figure 50.Scratch Test of RUN91

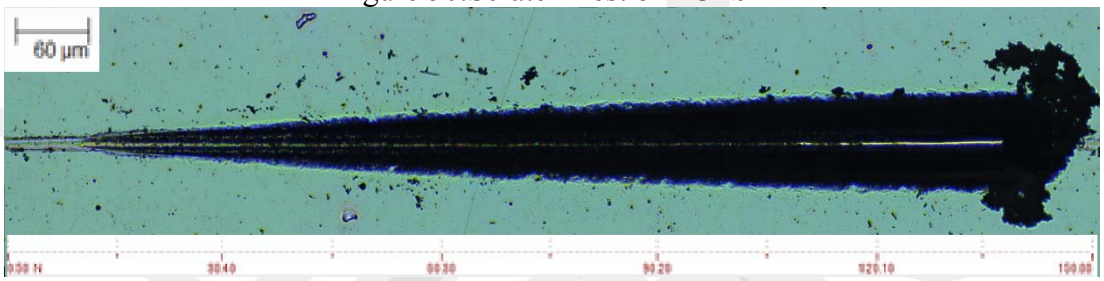

Figure 51.Scratch Test of RUN79

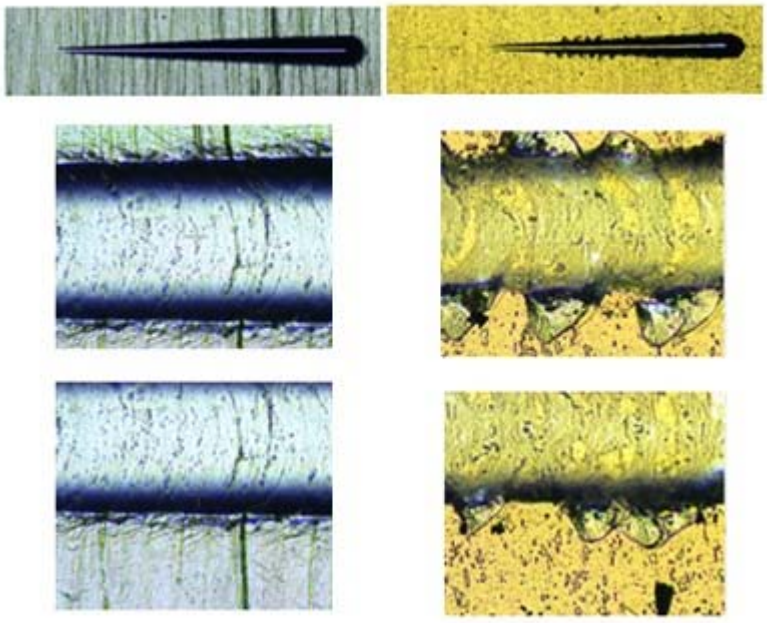

Figure 52. BN (a) and TiN (b) Steel Sample for Surface Adhesion

6.3. Hardness Measurements

Hardness is used to characterize the mechanical properties of materials. To measure the hardness of the film, first substrate hardness is measured. Then, film is measured in order to compare with the parent material. The steel substrates are used for hardness measurements. A common rule about the critical penetration depth is that the penetration depth should be less than 10% of the film thickness [53]. The applied parameters are given in Table 7. 250mN and 1mN loadsare applied for these measurements.

Table 6.Nanohardness Measurement Parameters

Indenter Type	Berkovich
Material	Diamond
Loading Type	Linear
Approach Speed	3000nm/min
Maximum Load	250mN,1mN
Pause at Maximum Load	0,5 s and 0,1 s

		Uncoated stain
HIT (O&P)	Mean	8516,775
[MPa]	Max	8777,483
HVIT (O&P)	Mean	788,746
[Vickers]	Max	812,890
hm (O&P)	Mean	1193,233
[nm]	Max	1213,974

Figure 53.Nanohardness test of uncoated samples

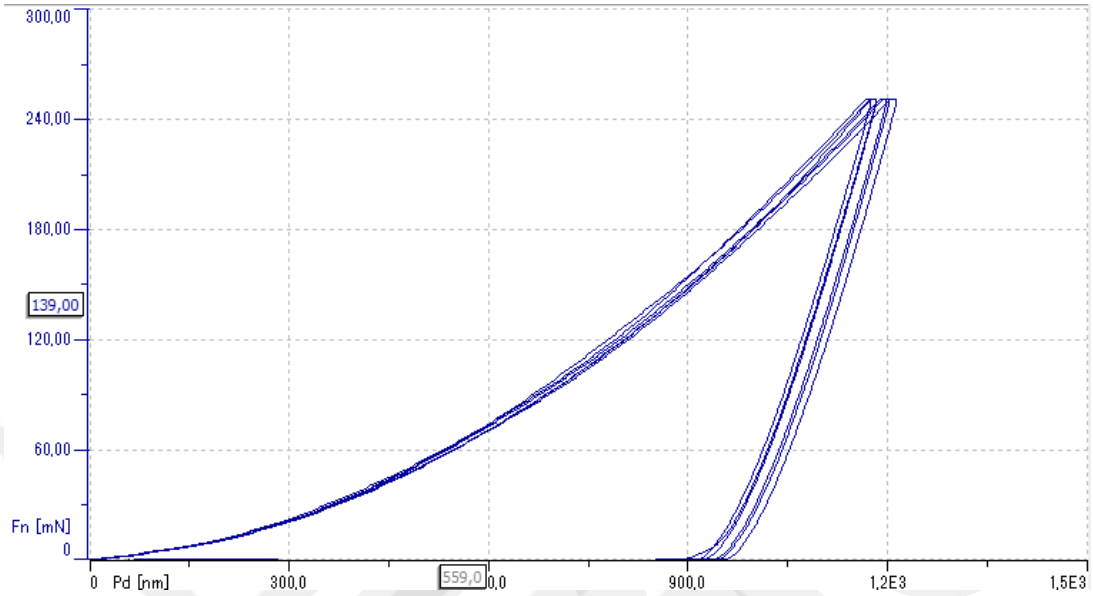

Figure 54.Pd- Fn graphs of uncoated steel

250 mN load is applied on uncoated steel sample to determined which load should be applied from the graph (Fig. 54). The uncoated steel samples hardness is 8GPa (850 Vickers). Coated samples are measured at 1mN load. From the results, the maximum hardness is reached atRUN40, RUN41, RUN69, RUN95, RUN 103, RUN 113coatings that is applied maximum substrate bias voltage which is at 250V. The highest hardness value is 18.75 GPa. Ultimately, the average of the film hardness is 15,87 GPa at 1 mN.

The minimum hardness is obtained at RUN89, RUN92, RUN 93, RUN 96, RUN99, RUN 100, RUN 117, RUN 108, RUN 109, RUN 110, RUN 112, RUN 114, RUN 116, RUN 117, RUN 118, RUN 120, RUN 122. In these experiments voltage is applied 1 hour 100V and 5 hours without substrate bias. In conclusion, average hardness is 4,24 GPa at 1mN load. This results show that this coating parameter encourages the growth of the h-BN allotrope.

According to the observed results, substrate bias voltage plays an important role in hardness. Increasing the voltage can be result in hard coatings. Furthermore, the resulting low hardness brings with a high thickness. Detail results aregiven in Appendix III.

Another parameter is microwave effect which affects the hardness.While the average hardness is 5 GPa using microwave effect at 0V, the average hardness is 3 GPa without using microwave effect at 0V. Hardness decreases according to using mw at 0V.

6.4. Friction Coefficient Measurements

Tribological behavior of magnetron sputtered BN coatings is investigated by use of ball-on-disk wear tester at 50mm/s and in load 1 N. Coated steel samples are used to evaluate friction coefficient measurements.In addition to this, the evaluation of the BN coatings, friction coefficient of the uncoated steel is also measured against alumina. Measurements results of the coefficient of friction is found to be 0,8 (Fig. 55). The friction coefficient of the BN coated samples is 0,4-0,5. The main parameter of the evaluation is thickness. Time scale and distance scale changes according to thickness.

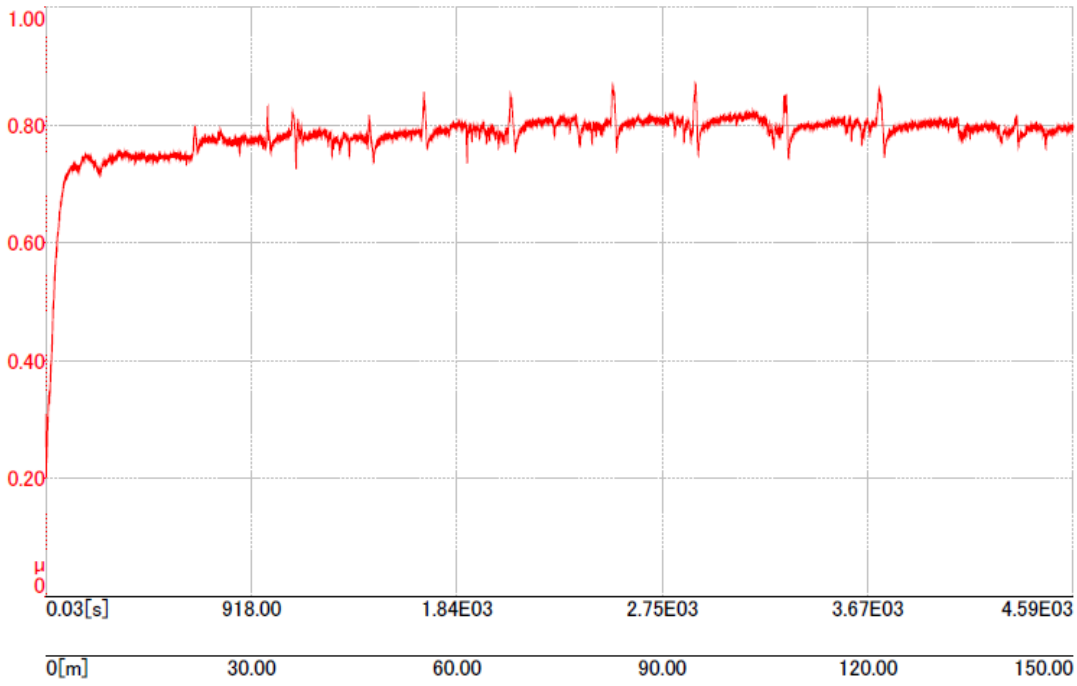

Figure 55.Friction coefficient results of uncoated steel

RUN31 has long time and distance scale. Also, RUN31 has lowest friction coefficient and its thickness is approximately 900 nm with hardness 4GPa (Fig. 56). RUN89 has long distance scale and time scale and its thickness is approximately 1-2µm and its hardness is 9GPa (Fig. 58). RUN91 has lowest time scale and it has also lowest thickness (Fig. 57). All measurements results are given in Appendix VI.

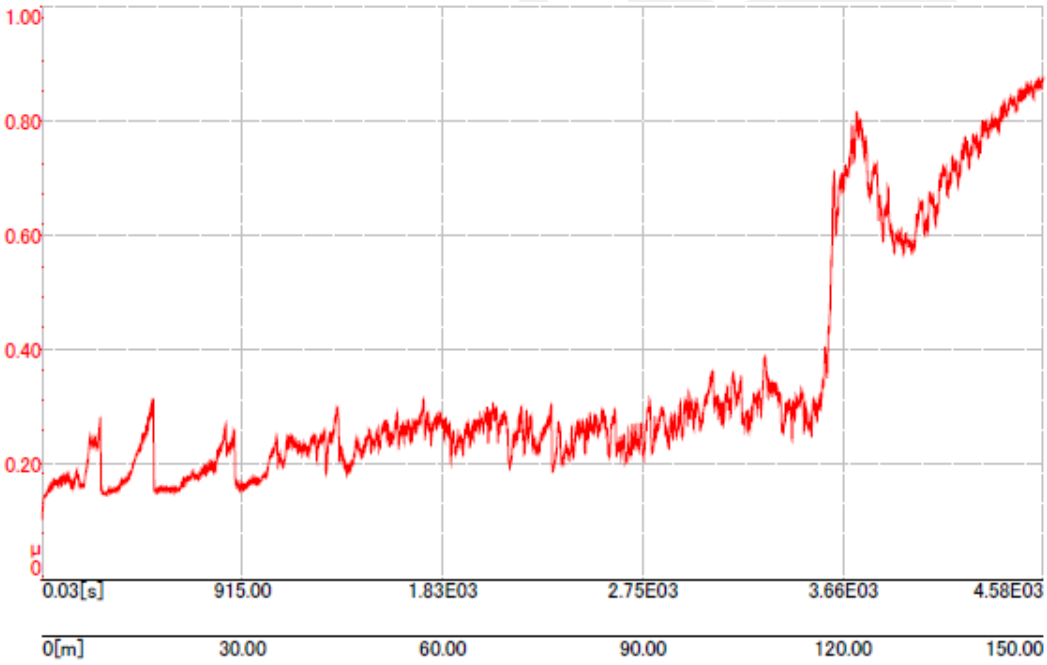

Figure 56. Friction Coefficient Result of RUN31

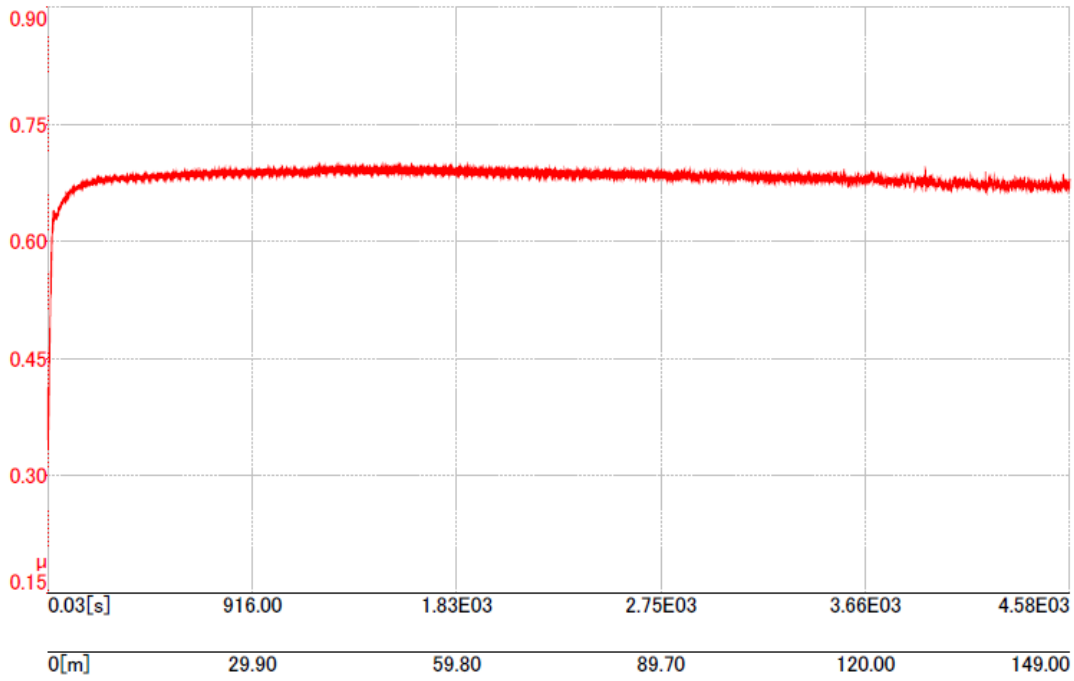

Figure 57. Friction Coefficient Result of RUN91

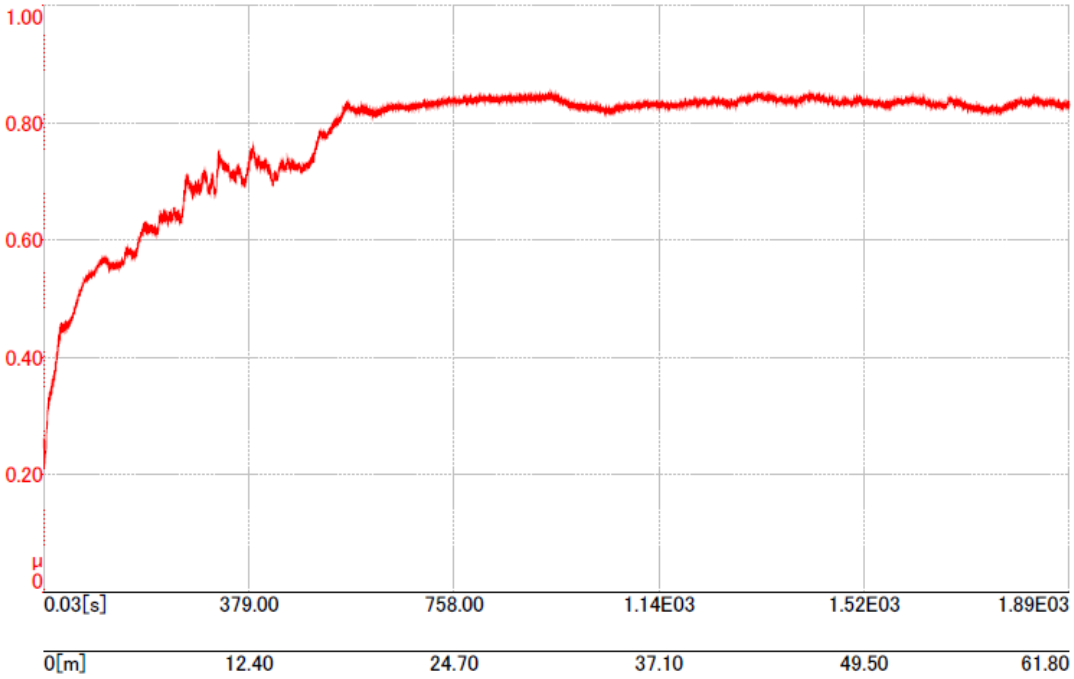

Figure 58. Friction Coefficient Result of RUN89

6.5. Fourier Transform Infrared Spectroscopy (FTIR) Measurements

Coated BN films are examined by FTIR in terms of crystal structure. BN films have many allotropes and among the most desirable ones is the cubic structure (c-BN) because of its exceptional properties. FTIR analysis is applied to all samples.The absorption mode is used to investigate the crystal structure of BN thin film coatings. Cumulative peaks are deconvolutedusing "Origin"software which is data analyzing software. FTIR is a nondestructive technique for thin films used for structural analyses.

FTIR spectra for BN thin film coatings are given in Table 7. All coating materials exhibit two major bands at about ~700 cm^{-1} and ~1360 cm^{-1} which is characteristic of h-BN [54]. In addition to this, a broad peak which can be seen in the same Figure 59 around wavenumber 1082 $cm^{-1}$is analyzed by peak fitting method which can be assigned to c-BN. In the same spectra there is another peak at 1470 cm^{-1} which might be associated with e-BN [26] and at about ~960 cm^{-1} and ~1270 cm^{-1} accepted as a w-BN and a-BN, respectively (Fig. 59).h-BN is highly observed some samples such as RUN 76 (Fig.61). w-BN is highly observed some samples such as RUN 92 (Fig. 62). Absorption bands of BN are given in Table 10. More research is needed to understand, more deeply, physical and optical properties of BN allotropes.

Table 7.IR absorption band of BN

Phases of BN	**Peak Range (cm^{-1})**
hBN bending	760–800
hBN stretching (TO)	1364–1400
h-BN stretching (LO)	1600
c-BN stretching (TO)	1055–1110
c-BN stretching (LO)	1300
a-B:N	1263–1350
a-B:N	1505–1550
w-BN (TO)	960, 1090, 1120, 1230
w-BN (LO)	1150, 1250
e-BN	1400-1450 (s),
	1650-1600, 1100,
	1020, 930 (ms),
	800, 1200 (vw)
r-BN (TO)	783, 1367
r-BN (LO)	828, 1610
t-BN	934.3,963.8,1331.8
t-BN	738,1032,1155

Various thin film deposition techniques have been suggested so far including physical and chemical deposition process. According to Samantray et al. c-BN film is composed of three layered structure a-BN (*amorphous*) layer, t-BN (*turbostratic*) layer and finally a c-BN (*cubic*) layered structure.

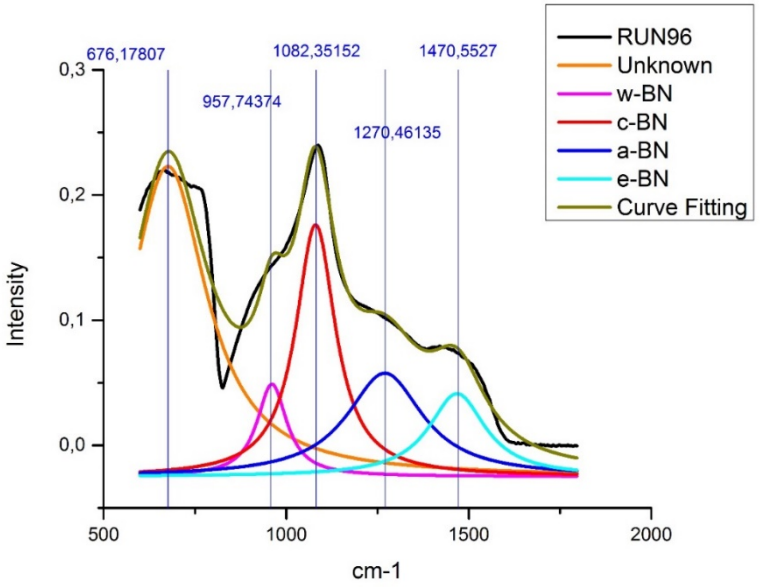

Figure 59. FTIR analysis result of RUN 96

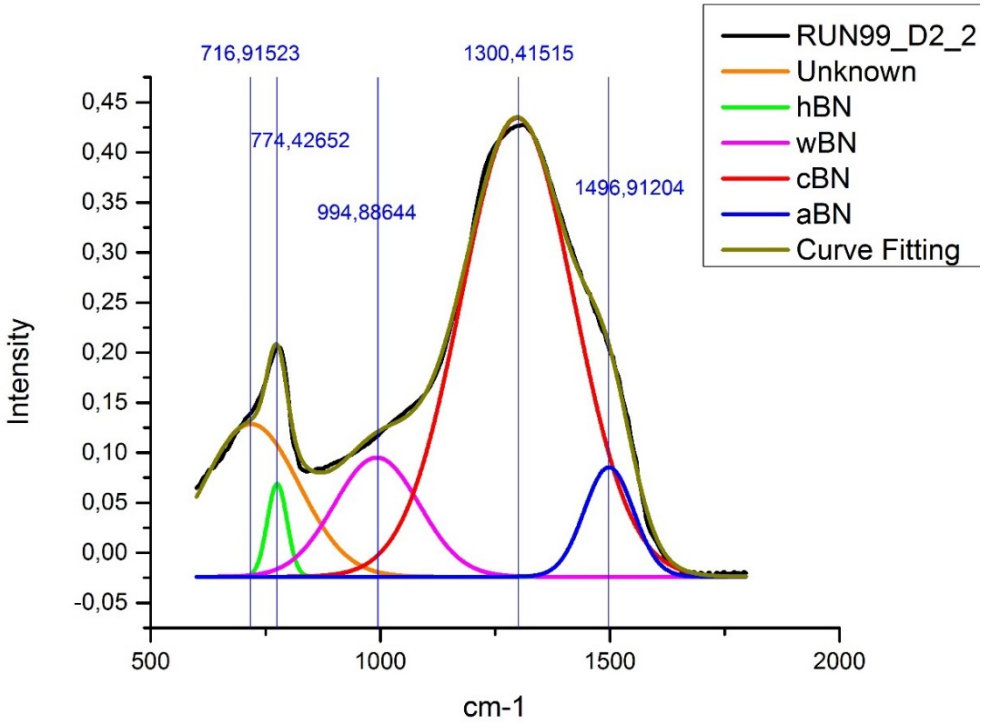

Figure 60. FTIR analysis result of RUN 99

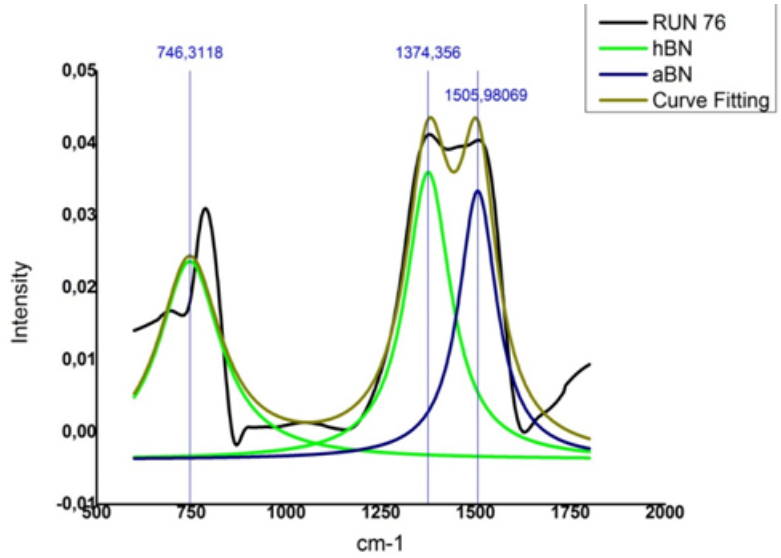

Figure 61.FTIR analysis result of RUN 76

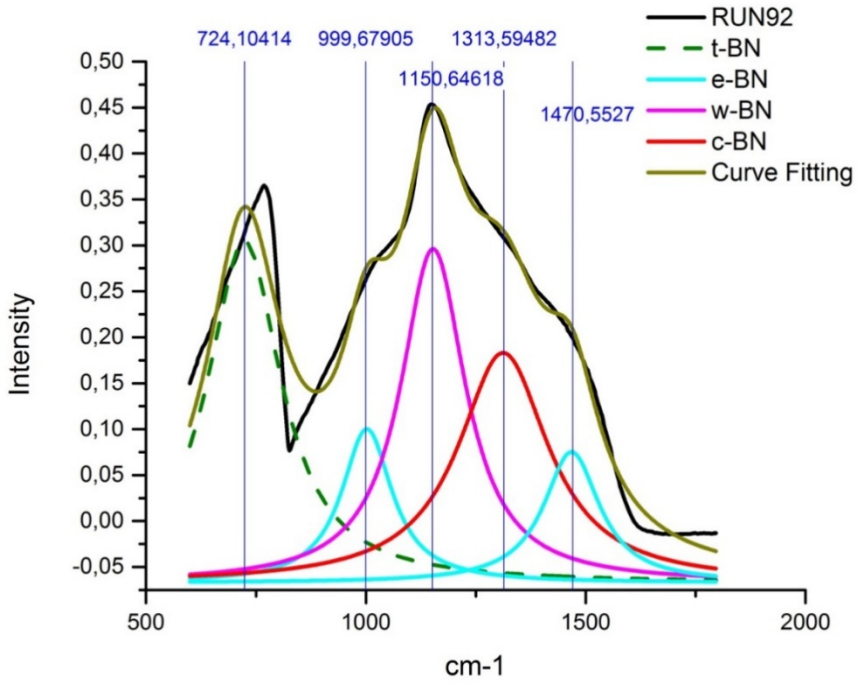

Figure 62. FTIR analysis result of RUN 92

6.6. Experiments Conducted for Industry

- **Dies**

Dies were also coated for industry. These substrates are made of powder metallurgy steel and are coated with different material before BN coating. Coated types are TiN, AlCrN, CrN and AlTiN. From coated dies, only thickness could be measured. Other characterization tests were performed on samples of the die steel. According to Figure 63, BN is coated on CrN has the highest thickness.

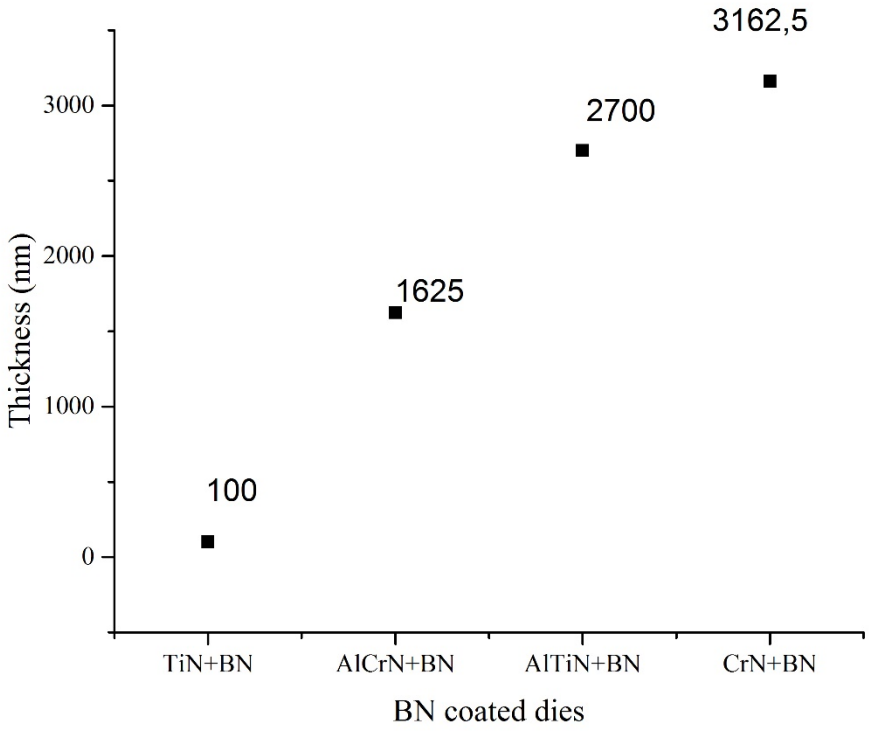

Figure 63. BN coated dies vs. thickness

These coated dies have been tried in industry and their performance increased. In addition, according to the experiments in industry, the life of coated dies has been reported to have increased by 2,5 times. Uncoated dies were also coated by BN coatings with different substrate bias voltage. In this experiment, the best thickness film is obtained at (100+0) V also resulting in best wear life (Fig. 64).

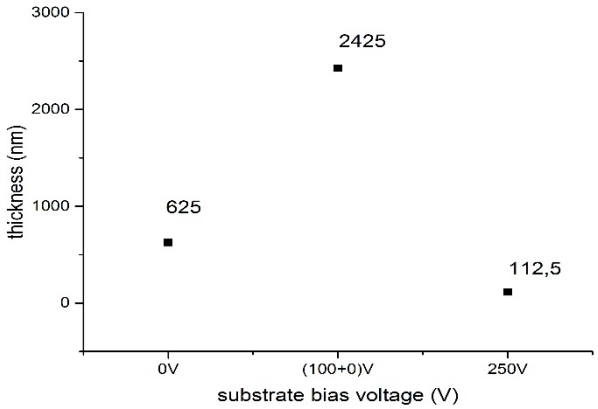

Figure 64. Thickness vs. different substrate bias voltage on uncoated die steels

- **Bearing Rings**

The other study for industry is coating the bearing rings. Rings are coated during 54 hours. Time effect and also substrate differences were investigated.

In some experiments, by changing the deposition time the effects of time were examined. Bearing rings were coated for industry. According to Figure 65, thickness of bearing rings increase with increasing time is observed when substrate bias voltage is 0 V.

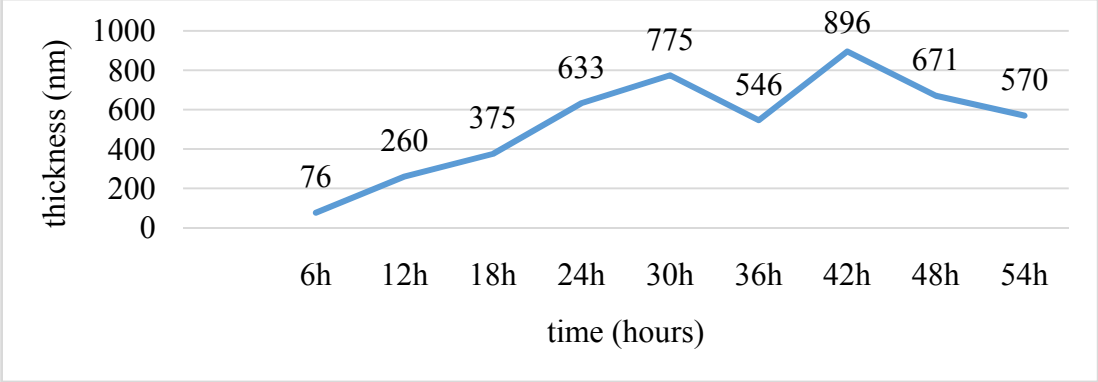

Figure 65. Time vs. thickness for bearing rings

Adhesion tests are performed only on D2 steels because of geometry of bearing rings and during the experiments, the substrate bias voltage is 0 V. The deposition time increases, the coating thickness increases. For this reason, cracks occurred when the deposition time increases in scratches (Fig. 66). These cracks may be caused by internal stresses.

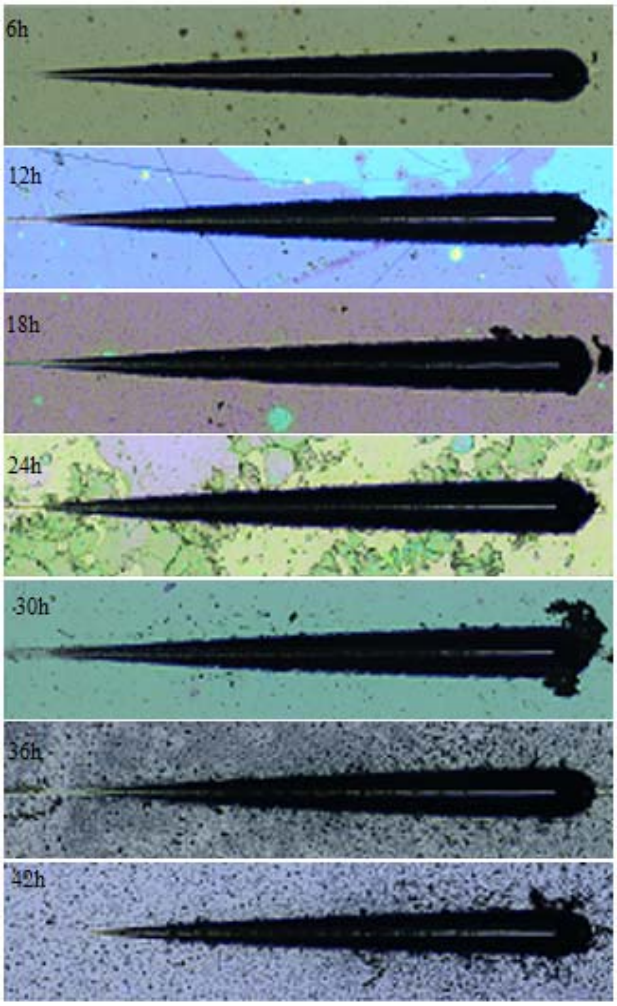

Figure 66.Time-dependent adhesion effect

Hardness tests are measured only on D2 steels like scratch measurements. As a result of the investigation, hardness of the steel (substrate) is measured around 7 GPa in the first 6 hours and at the end of the 54 hours, hardness is measured around 4 GPa at 250 mN.Time is also affected to hardness of the film. At 1mN load, film hardness is decreased. The lowest hardness is observed at the end of the 54 hours.

- The correlation between different substrate bias voltage and hardness and thickness

Considering all the results can be explained following charts. In this chart demonstrate that was observed hardness increases proportionally to the substrate bias voltage (Fig.67).

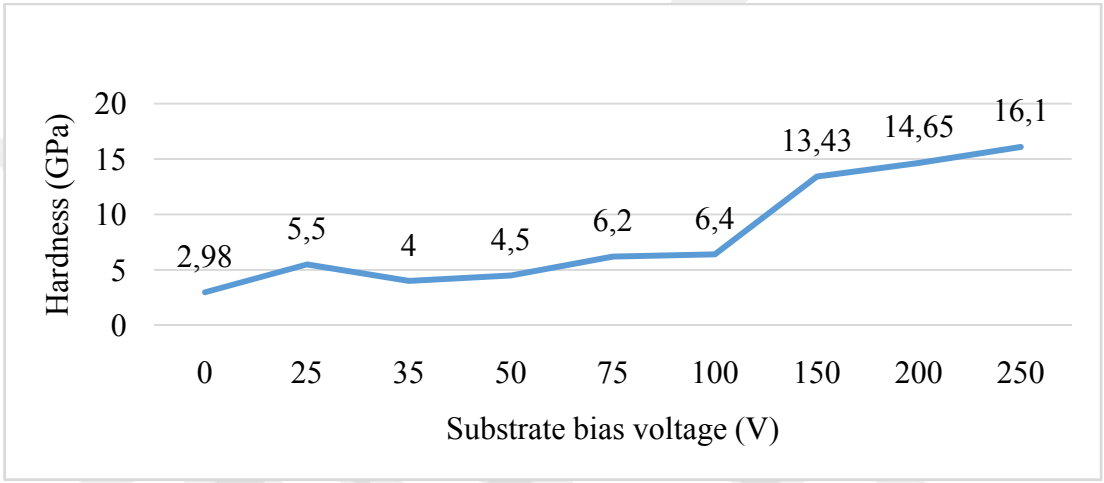

Figure 67. Substrate bias voltage vs. hardness

The thickness decreases as the voltage increases.(Fig. 68).

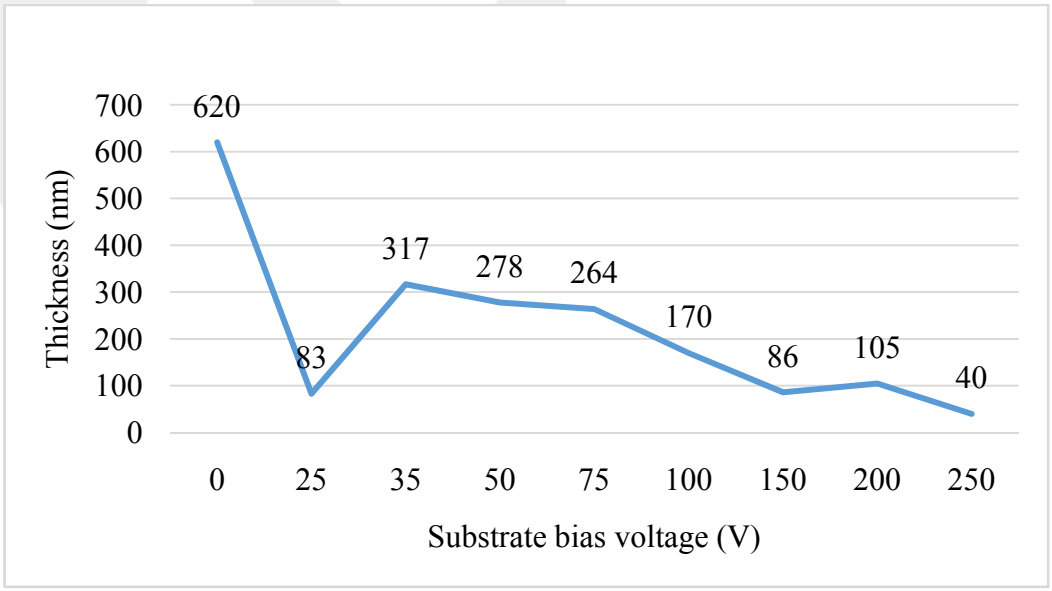

Figure 68. Substrate bias voltage vs. thickness

CHAPTER 7

CONCLUSION

BN films deposited through magnetron sputtering method without hydrogen gas and applied bias voltagewere fully characterized. Sample characterization with FTIR was done to determine phase formation. Nanohardness was used to determine film hardness. Scratch testwas performed for adhesion quality. Filmetrics® was applied to measure thickness of thin film. The tribological test of the sample deposited for generally 6 hours at 300°C measured the BN film friction coefficient. Magnetron power is 900 W and is stable during this research. This research is performed under $5x10^{-3}$Torr. Substrate bias voltage is changed from 0 to 250V. Approximately a hundred tests are examined.

The analyses applied to the samples in this investigation can be classified by parameters of substrate bias voltage, spindle mechanism and different substrates

i) Samples deposited for one hour with 100V followed by five hours with 0V (substrate bias)– without using the spindle mechanism - were characterized by FTIR, thickness, hardness, adhesion test. Some phase formation of BN is shown in the infrared spectra. The highest thickness is obtained in this parameter. On the other hand, the hardness was relatively reduced. BN film thickness reached 4 microns.Adhesion gained a little homogeneity.

ii) Samples deposited for one hour with 100V followed by five hours at 0V (substrate bias) with spindle mechanism runningwere characterized by FTIR, thickness, hardness, adhesion test. All BN allotropes are obtained in varying proportions. Thickness showed a decreasedown to half a micron thickness. Adhesion improved.

iii) Samples deposited at maximum voltage (250 V bias voltage) were characterized by FTIR, thickness, hardness, adhesion test. Highest hardness is reached with a low thickness of the coated film.

iv)Gas ratio is also another parameter during the process. Grown BN films with different gas ratios showed nearly the same behavior.

v) Different(substrates) dies are deposited with the same substrate voltage (100+0) Vbias. Coating on powder metallurgy steel samples were characterized by FTIR, thickness, hardness, adhesion test. Dies are coated with various coatings such as TiN, AlTiN, AlCrN and CrN. Also, some dies are uncoated like die steel. The thickness measurements are performed by Filmetrics®. BN films were grown from 100nm to 4µm on dies. Using coated die steels, according to the press amount of dies and take into account its changes are examined to performance.

vi) Experiment time is another parameter of coating. Thickness increases while time increases. Depending on the increasing thickness, some cracks appeared in adhesion test.

vii) Further research is necessary to find out properties of BN allotropes for analyzing to BN phases. FTIR results demonstrate that all BN phases are obtained in various proportion.

As a result of all coating measurement from different parameters, it is observed that substrate V (bias) has positive effect to thickness. The best V(bias) is (100+0) V.

CHAPTER 8

FUTURE WORK

In the light of this study, future samples can be deposited with hydrogen gas to achieve cubic phase. To achieve a uniform film, physical deposition parametershave to be investigated. During the deposition, contaminants can affect the deposition quality.Multi-layered coating can be optimized with different target plates. Crystal structure of BN can be investigated in detail. An interesting analysis could be done at the interlayers ofphases to understand the transformation from hexagonal to cubic phase.

Thin film studies improved in direct or indirectly a lot of new areas of research.

Current system has some limitations. Due to these limitations high surface energy cannot be studied. High surface energy provides a higher percentage of cubic boron nitride. It will be possible to coat samples andindustrial parts with high quality surface properties resulting in superior wear resistance, hardness and adhesion characteristics.

For the future work, parameters of experiments may be optimized to obtain higher hardness and more wear resistance.Internal stress of the film can cause delamination. This effect can be investigated by measurements.

REFERENCES

[1] Habashi, F. (2015). A New Look at The Periodic Table. European Chemical Bulletin, 4(1-3), 1-7.

[2] BOREN National Boron Research Institute "The Boron Element". www.boren.gov.tr/en/boron/boron-element, 10 October 2015.

[3] "Boron: the essentials", http://www.webelements.com/boron/, 2015.

[4] "Boron", http://tarek.kakhia.org, 2015.

[5] Li, N., Li, X., Geng, W., Zhao, L., Zhu, G., Wang, R., & Qiu, S. (2005). Template synthesis of boron nitride nanotubes in mesoporous silica SBA-15.Materials Letters, 59(8), 925-928.

[6] Taylor II, C. A., & Clarke, R. (1997). Growth kinetics of cubic boron nitride films and composites. In Diamond Based Composites (pp. 63-113). Springer Netherlands.

[7] Kumashiro Y. (2000). Electric Refractory Materials, CRC Press.

[8] Haubner, R., Herrmann, M., Lux, B., Petzow, G., Weissenbacher, R., & Wilhelm, M. (2003). High performance non-oxide ceramics II (Vol. 102). M. Jansen (Ed.). Springer.

[9] Mirkarimi, P. B., McCarty, K. F., & Medlin, D. L. (1997). Review of advances in cubic boron nitride film synthesis. Materials Science and Engineering: R: Reports, 21(2), 47-100.

[10] Souche, C., Jouffrey, B., Hug, G., & Nelhiebel, M. (1998). Orientation sensitive EELS-analysis of boron nitride nanometric hollow spheres. Micron, 29(6), 419-424.

[11] Balmain, W. H. (1842). Bemerkungen über die Bildung von Verbindungen des Bors und Siliciums mit Stickstoff und gewissen Metallen. Journal für Praktische Chemie, 27(1), 422-430.

[12] Yurasova, V. E., Elovikov, S. S., & Zykova, E. Y. (2007). Sputtering of boron nitride single crystals of different structure. Journal of Surface Investigation. X-ray, Synchrotron and Neutron Techniques, 1(3), 328-341.

[13] Sung, C. M., & Tai, M. F. (1995). Mechanism of the solvent-assisted graphite to diamond transition under high pressure: implications for the selection of catalysts. High Temperatures. High Pressures, 27(5), 523-546.

[14] Kaftanoğlu, B., & Dökmetaş, N. (2014). An environmentally friendly method of cutting and forming of materials by boron nitride coated tools. International Journal of Sustainable Manufacturing 10, 3(2), 143-155.

[15] KopeliovichD., (2012). http://www.substech.com/dokuwiki/doku.php?id=boron_nitride_as_solid_lubricant.

[16] Band structure and carrier concentration (1996). http://www.ioffe.ru/SVA/NSM/Semicond/BN/bandstr.html.

[17] Wentorf, R. H., De Vries, R. C., & Bundy, F. P. (1980). Sintered superhard materials. Science, 208(4446), 873-80.

[18] Zhu, P. W., Zhao, Y. N., Wang, B., He, Z., Li, D. M., & Zou, G. T. (2002). Prepared low stress cubic boron nitride film by physical vapor deposition.Journal of Solid State Chemistry, 167(2), 420-424.

[19] Vel, L., Demazeau, G., & Etourneau, J. (1991). Cubic boron nitride: synthesis, physicochemical properties and applications. Materials Science and Engineering: B, 10(2), 149-164.

[20] Uhlmann, E., Fuentes, J. O., & Keunecke, M. (2009). Machining of high performance workpiece materials with CBN coated cutting tools. Thin solid films, 518(5), 1451-1454.

[21] Kumashiro, Y. (2000). Electric refractory materials. CRC Press.

[22] Zuckerman, J. J. (2009). Inorganic Reactions and Methods, Formation of Bonds to Transition and Inner-Transition Metals (Vol. 14). John Wiley & Sons.

[23] Monteiro, S. N., Skury, A. L. D., de Azevedo, M. G., & Bobrovnitchii, G. S. (2013). Cubic boron nitride competing with diamond as a superhard engineering material–an overview. Journal of Materials Research and Technology, 2(1), 68-74.

[24] Zhu, P. W., He, Z., Zhao, Y. N., Li, D. M., Liu, H. W., & Zou, G. T. (2002). Preparation of high-pressure phase boron nitride films by physical vapor deposition. Journal of Vacuum Science & Technology A, 20(3), 622-624.

[25] Bello, I., Chong, Y. M., Leung, K. M., Chan, C. Y., Ma, K. L., Zhang, W. J.,& Layyous, A. (2005). Cubic boron nitride films for industrial applications.Diamond and related materials, 14(11), 1784-1790.

[26] Mirkarimi, P. B., McCarty, K. F., & Medlin, D. L. (1997). Review of advances in cubic boron nitride film synthesis. Materials Science and Engineering: R: Reports, 21(2), 47-100.

[27] Ulrich, S., Nold, E., Sell, K., Stüber, M., Ye, J., & Ziebert, C. (2006). Constitution of thick oxygen-containing cubic boron nitride films. Surface and Coatings Technology, 200(22), 6465-6468.

[28] Yu, W. J., Lau, W. M., Chan, S. P., Liu, Z. F., & Zheng, Q. Q. (2003). Ab initio study of phase transformations in boron nitride. Physical Review B, 67(1), 014108.

[29] Grinyaev, S. N., & Lopatin, V. V. (1997). Chemical bond and electronic structure anisotropies in the graphitic and rhombohedral modifications of boron nitride. Journal of structural chemistry, 38(1), 25-33.

[30] Wurtzite Boron Nitride (2015). http://www.everystockphoto.com/photo.php?imageId=1668695.

[31] Batzanov S.S., Blochin G. E. & Deribas A. A. (1965) J. Struct. Chem. 7, 209.

[32] Akashi, T., Sawaoka, A., Saito, S., & Araki, M. (1976). Structural changes of boron nitride caused by multiple shock-compressions. Japanese Journal of Applied Physics, 15(5), 891.

[33] Sokołowski, M., Sokołowska, A., Michalski, A., Romanowski, Z., Rusek-Mazurek, A., & Wronikowski, M. (1981). The deposition of thin films of materials with high melting points on substrates at room temperature using the pulse plasma method. Thin Solid Films, 80(1-3), 249-254.

[34] Sokotowska, A; Olszyna, A, Electron assisted chemical synthesis of E-BN,Journal of crystal growth,116,3-4,507-510,1992,North-Holland.

[35] Biscoe, J., & Warren, B. E. (1942). An X-Ray Study of Carbon Black. Journal of Applied Physics, 13(6), 364-371.

[36] 36- Warren, B. E. (1941). X-ray diffraction in random layer lattices. Physical Review, 59(9), 693.

[37] Zuckerman, J. J., Hagen, A. P., Norman, A. D., & Atwood, J. D. (1999). Inorganic Reactions and Methods, Cumulative Index: Author and Subject Indexes (Volumes 1-18).

[38] Zedlitz, R., Heintze, M., & Schubert, M. B. (1996). Properties of amorphous boron nitride thin films. Journal of non-crystalline solids, 198, 403-406.

[39] Pouch, J. J., Alterovitz, S. A., & Warner, J. D. (1986). Auger electron spectroscopy, secondary ion mass spectroscopy and optical characterization of aCH and BN films.

[40] Nistor, L., Dinca, G., Balint, M., & Petrescu, M. (2002). Cubic Boron Nitride-- Properties, Preparation, Applications, Market Trends Part I- Structure and Properties of Cubic Boron Nitride. UPB Buletin Scientifics, Series B: Chemistry and Materials Science, 64(1), 51-60.

[41] Yu, W. J., Lau, W. M., Chan, S. P., Liu, Z. F., & Zheng, Q. Q. (2003). Ab initio study of phase transformations in boron nitride. Physical Review B, 67(1), 014108.

[42] Mattox, D. M. (2010). Handbook of physical vapor deposition (PVD) processing. William Andrew.

[43] Moarrefzadeh, A., & Branch, M. (2012). Simulation and Modeling of Physical Vapor Deposition (PVD) Process. Wear Transactions on Applied and Theoretical Mechanics, 7(2).

[44] Mattox, D. M. (1998). Handbook of physical vapor deposition (PVD) processing.

[45] Lieberman, M. A., & Lichtenberg, A. J. (2005). Principles of plasma discharges and materials processing. John Wiley & Sons.

[46] Ekpe, S. D., & Dew, S. K. (2008). Energy deposition at the substrate in a magnetron sputtering system. In Reactive Sputter Deposition (pp. 229-254). Springer Berlin Heidelberg.

[47] Hallman Robert, A Study of TiN Coatings on Medical Implants Deposited by HiPIMS, Master of Science in Engineering Technology Engineering Physics.

[48] Kempe, P. (2011), CSM Instruments, "New Applications and Products Applications and Measurements.

[49] Vaughn, G. D., Frushour, B. G., & Dale, W. C. (1994). Scratch indentation, a simple adhesion test method for thin films on polymeric supports. Journal of adhesion science and technology, 8(6), 635-650.

[50] Oliver, W. C., & Pharr, G. M. (1992). An improved technique for determining hardness and elastic modulus using load and displacement sensing indentation experiments. Journal of materials research, 7(06), 1564-1583.

[51] Oliver, W. C., & Pharr, G. M. (2004). Measurement of hardness and elastic modulus by instrumented indentation: Advances in understanding and refinements to methodology. Journal of materials research, 19(01), 3-20.

[52] Yamada, Y., Tatebayashi, Y., Tsuda, O., & Yoshida, T. (1997). Growth process of cubic boron nitride films in bias sputter deposition. Thin Solid Films, 295(1), 137-141.

[53] Klimczyk, P., Figiel, P., Petrusha, I., & Olszyna, A. (2011). Cubic boron nitride based composites for cutting applications. Journal of Achievements in Materials and Manufacturing Engineering, 44(2), 198-204.

[54] Samantaray, C. B., & Singh, R. N. (2005). Review of synthesis and properties of cubic boron nitride (c-BN) thin films. International materials reviews, 50(6), 313-344.

[55] Bückle, H. (1959). Progress in micro-indentation hardness testing. Metallurgical Reviews, 4(1), 49-100.

[56] Yu, L., Gao, B., Chen, Z., Sun, C., Cui, D., Wang, C.,& Jiang, M. (2005). In situ FTIR investigation on phase transformations in BN nanoparticles. Chinese Science Bulletin, 50(24), 2827-2831.

[57] Inspektor, A., & Salvador, P. A. (2014). Architecture of PVD coatings for metalcutting applications: a review. Surface and Coatings Technology, 257, 138-153.

[58] Vel, L., Demazeau, G., & Etourneau, J. (1991). Cubic boron nitride: synthesis, physicochemical properties and applications. Materials Science and Engineering: B, 10(2), 149-164.

[59] H. Holleck, "Advanced concepts in PVD hard coating", Metall., vol. 43, no. 7, pp. 614-624, 1989.

[60] BOREN National Boron Research Institute (2015). “The Boron Element”. www.boren.gov.tr/en/boron/boron-element.

[61] Nitrogen: electronegativity (2015), www.webelements.com/nitrogen/electronegativity.html

[62] Kurdyumov, A. V., Solozhenko, V. L., Zelyavsky, W. B., & Petrusha, I. A. (1993). The structural aspect of wurtzite boron nitride phase stabilization.Journal of Physics and Chemistry of Solids, 54(9), 1051-1053.

[63] Wakatsuchi, M., Takaba, Y., Ueda, Y., & Nishikawa, M. (1999, December). Boron nitride film deposition by reactive sputtering with ECR plasma. In Ion Implantation Technology Proceedings, 1998 International Conference on (Vol. 2, pp. 748-751). IEEE.

[64] Clausing, R. E., Horton, L. L., Angus, J. C., & Koidl, P. (Eds.). (2012). Diamond and diamond-like films and coatings (Vol. 266). Springer Science & Business Media.

[65] Boron Report, (2015). www.kimyamuhendisi.org

[66] Poon, B., Rittel, D., & Ravichandran, G. (2008). An analysis of nanoindentation in linearly elastic solids. International Journal of Solids and Structures, 45(24), 6018-6033.

APPENDIX I

PUBLICATIONS

List of Publications (in chronological order)

1. B. Kaftanoğlu, N. Dökmetaş, A. E. S. Özhan, T. Hacaloğlu, M. Kılıçkan (2014), "On Boron Nitride Coating of Metals", Nano Studies, 2014, 10, 3-4, p:21-28
2. B. Kaftanoğlu, N. Dökmetaş, A. E. S. Özhan, T. Hacaloğlu, M. Kılıçkan "On Boron Nitride Coating of Metals" NANO – 2014
3. B. Kaftanoğlu, N. Dökmetaş, A. E. S. Özhan, T. Hacaloğlu, M. Kılıçkan "Surface Properties of Boron Nitride Coatings" ECOSS 30, Antalya 2014
4. B.Çetin, O.Kırıcıoğlu, E.Köseoğlu, N.Dökmetaş, T.Hacaloğlu, M.Kılıçkan, B.Kaftanoğlu, "Tool Life Improvement of End Mill Cutters with BN Coating by PVD Method ", 8th International Conference and Exhibition on Design and Product of Machines and Dies/Molds, p:211-216, 2015
5. I.O.Yılmaz ,B.Kaftanoglu,T. Hacaloglu, M. Kılıckan "Integration of Press Hardening with Cold Trimming" ,5 ICAFT/22 SFU 2015, 105-118, 2015

APPENDIX II

SUPPORTERS & COLLABORATORS

SUPPORTERS

1. ATILIM UNIVERSITY

   Project No: ATÜ-BAP-A-1213-02

2. TUBITAK (Scientific and Technological Council of Turkey)
   Research No: 114S391

LABORATORIES

1. BOREN CENTER of COMPETENCE for BORON COATING
2. METAL FORMING CENTER of EXCELENCE

INDUSTRY

1. VAKSIS R&D Engineering, Turkey
2. ANTON PAAR GmbH

APPENDIX III

HARDNESS MEASURMENTS

Hardness measurement results at 250mN

	250mN						
		MPa		***Vickers***		***hm(nm)***	
	#I	***Mean***	***Max***	***Mean***	***Max***	***Mean***	***Max***
RUN1	9	9050.903	9609.475	838.212	889.942	1188.143	1216.584
RUN2	10	9394.747	9996.313	870.056	925.767	1165.569	1189.079
RUN3	10	9033.611	11135.822	836.611	1031.298	1189.947	1235.303
RUN4	10	9807.741	11868.084	908.304	1099.114	1143.213	1206.816
RUN5	10	10803.687	15395.019	1000.539	1425.746	1118.343	1263.698
RUN6	8	5839.438	6619.743	540.795	613.060	1436.709	1508.282
RUN7	9	14875.464	17325.820	1377.630	1604.559	1015.849	1498.803
RUN8	10	6482.031	6865.976	600.307	635.864	1366.441	1390.804
RUN9	10	7591.349	8809.359	703.041	815.843	1289.518	1523.801
RUN10	10	5243.921	6204.644	485.644	574.617	1502.476	1681.151
RUN11	8	7005.322	7361.694	648.769	681.773	1325.470	1349.731
RUN12	1	7731.208	7731.208	715.994	715.994	1269.824	1269.824

RUN13	1	9280.998	9280.998	859.521	859.521	1186.751	1186.751
RUN14	1	8285.854	8285.854	767.360	767.360	1235.554	1235.554
RUN15	1	2790.031	2790.031	258.387	258.387	2016.035	2016.035
RUN16	1	4893.794	4893.794	453.219	453.219	1560.357	1560.357
RUN17	1	8674.114	8674.114	803.317	803.317	1230.719	1230.719
RUN18	1	7706.011	7706.011	713.660	713.660	1262.122	1262.122
RUN19	1	12863.473	12863.473	1191.297	1191.297	1044.493	1044.493
RUN20	1	6831.233	6831.233	632.647	632.647	1343.780	1343.780
RUN21	1	9084.541	9084.541	841.327	841.327	1183.144	1183.144
RUN22	1	6814.104	6814.104	631.060	631.060	1333.214	1333.214
RUN23	1	1657.226	1657.226	153.477	153.477	2595.026	2595.026
RUN24	1	7972.927	7972.927	738.380	738.380	1260.169	1260.169
RUN25	10	8558.610	10619.174	792.621	983.451	1211.402	1399.339
RUN26	10	17884.590	47827.449	1656.308	4429.342	1010.731	1218.020
RUN27	1	5111.432	5111.432	473.374	473.374	1535.944	1535.944
RUN28	10	5691.766	6819.766	527.120	631.492	1498.434	1926.130
RUN29	10	4160.858	5796.204	385.341	536.792	1728.258	2002.450
RUN30							
RUN31	10	7483.456	8028.569	693.049	743.533	1315.115	1574.340
RUN32	10	9045.708	11707.040	738.731	1084.199	1202.569	1335.581
RUN33	10	5751.247	6761.124	532.628	626.154	1478.821	1577.188
RUN34	10	16553.174	20626.389	1533.004	1910.228	962.277	1041.828
RUN35_D2	10	15719.264	23936.424	1455.775	2216.773	1106.621	2568.906
RUN35_TINKAP	10	12263.295	14851.064	1135.715	1375.370	1056.236	1084.344
RUN36							
RUN37							

RUN38	10	16522.797	19337.135	1530.191	1790.829	955.910	1051.159
RUN39	10	16425.623	23385.434	1521.192	2165.746	974.078	1094.093
RUN40	9	19182.039	28402.141	1776.465	2630.375	906.707	1018.273
RUN41	10	17338.277	24997.016	1605.713	2314.996	995.903	1408.986
RUN42	10	13097.008	21542.168	1212.926	1995.039	1426.956	3127.868
RUN43	10	16570.029	24837.246	1534.565	2300.199	966.724	1078.526
RUN44	10	16670.760	24740.521	1543.894	2291.242	963.202	1146.468
RUN45	10	15360.252	19894.615	1422.526	1842.458	993.709	1134.057
RUN46	10	18593.137	22851.914	1721.927	2116.336	923.813	1027.766
RUN47	9	16339.741	31357.654	1513.238	2904.060	1023.858	1636.159
RUN48	10	16010.731	18643.572	148.768	1726.598	975.189	1030.423
RUN49	10	11421.056	16787.795	1057.714	1554.732	1059.933	1227.969
RUN50	10	1175.582	12779.461	1034.981	1183.517	1095.362	1129.714
RUN51	10	8348.638	15392.650	773.175	1425.527	1356.566	2660.855
RUN52-D2	10	10439.035	12025.210	966.768	1113.665	1129.438	1261.444
RUN52-Ti	9	12434.086	15884.887	1151.532	1471.113	1052.552	1095.195
RUN53	10	16289.685	18288.076	1508.324	1693.675	951.914	1002.161
RUN54	9	9218.627	11554.828	853.745	1051.581	1186.725	1234.949
RUN55	10	9394.678	10819.593	870.049	1002.012	1175.769	1227.739
RUN56	10	8142.380	13148.057	754.073	1217.653	1267.250	1344.410
RUN57	8	7744.737	8049.587	717.247	745.479	1289.205	1312.118
RUN58	10	7658.139	8616.794	709.227	798.009	1319.337	1345.010
RUN59_B	10	13923.529	19150.725	1289.470	1773.566	1022.209	1123.118
RUN59	10	8626.658	9765.622	798.922	904.403	1218.075	1285.323
RUN60_B	10	7324.156	17225.641	678.297	1598.060	939.651	1304.232
RUN60	10	6191.071	12588.910	573.361	1165.870	1039.984	1408.682

RUN61	10	9151.526	11159.771	847.531	1033.516	1183.121	1233.527
RUN62	8	8337.732	8966.611	772.165	830.406	1247.929	1305.082
RUN63	10	7627.387	8180.818	706.379	757.633	1293.699	1312.168
RUN64	10	4588.026	7904.309	424.901	732.025	1726.140	2236.777
RUN65	10	12311.842	13221.186	1140.210	1223.500	1070.834	1182.681
RUN66	10	1381.875	14627.806	1211.524	1354.694	1032.898	1063.592
RUN67_Bartın1	7	8106.546	8378.904	750.754	775.978	1264.687	1293.988
RUN68_Bartın2	8	8889.291	10128.346	823.245	937.995	1196.107	1237.950
RUN69_Bartın3	9	15558.953	16802.168	1440.928	1556.064	969.072	998.530
RUN70	10	6817.872	6964.775	631.409	645.014	1358.040	1397.050
RUN71	10	11098.146	17972.775	1027.809	1664.474	106.752	573.272
RUN72	9	13263.939	18822.697	1228.385	1743.187	1013.810	1079.873
RUN73	10	7471.537	9755.658	691.946	903.480	1286.423	1345.745
RUN74							
RUN75							
RUN76	7	6603.138	6832.464	611.523	632.761	1328.629	1343.148
RUN77	10	5865.124	6403.351	543.174	593.020	1412.900	1487.792
RUN78	9	4946.646	5120.758	458.113	474.238	1527.853	1550.545
RUN79	9	5038.556	5715.616	466.625	529.328	1517.071	1570.312
RUN80							
RUN81							
RUN82							
RUN83							
RUN84							
RUN85	9	5202.488	5381.723	481.807	498.406	1535.946	1554.236
RUN86	10	4889.274	5036.827	452.800	466.465	1581.089	1594.650

RUN87	10	4564.747	4664.201	422.745	431.956	1658.073	1670.798
RUN88	10	4310.313	4396.169	399.182	407.133	1706.149	1722.577
RUN89-Ti	10	4286.065	5012.284	396.936	464.192	1659.998	1784.135
RUN89-D2-1	8	7665,768	7872,908	709,934	729,117	1285,885	1300,094
RUN89-D2-2	10	7719,565	8049,385	714,916	745,461	1277,890	1299,029
RUN89-D2-3	4	2152,274	5788,350	199,324	536,064	2910,153	3523,281
RUN90-D2	9	6486.127	6715.276	600.686	621.908	1413.364	1444.006
RUN90-V1	6	7496.915	7636.987	694.296	707.268	1265.325	1278.569
RUN91-D2	8	11194.976	11955.040	1036.777	1107.167	1079.955	1112.412
RUN91-V2	4	18529.416	20491.314	1716.026	1897.719	894.134	974.362
RUN92	9	6887,990	7319,359	637,903	677,852	1388,590	1416,556
RUN93-D2	9	6738,917	7115,306	624,097	658,955	250,731	250,742
RUN93-V3	10	9178,376	9299,610	850,017	861,245	1181,492	1189,365
RUN95	10	16010,541	21110,500	1482,750	1955,062	957,077	1075,654
RUN96	7	7035,29	7442,897	651,544	689,293	1392,822	1424,762
RUN97	9	4938,845	5097,216	457,391	472,058	1657,027	1682,108
RUN98-D2	10	7360,125	7885,522	681,628	730,285	1300,207	1332,13
RUN98-V4	10	8544,842	8859,559	791,345	820,492	1233,084	1244,595
RUN99-D2	10	7214,194	7419,588	668,113	687,135	1302,783	1313,409
RUN99-V5	10	8509,152	8666,696	788,04	802,63	1235,394	1249,637
RUN100	10	7666,954	8040,376	710,043	744,626	1264,964	1287,372
RUN100-V6	10	9582,181	9928,576	887,414	919,494	1163,652	1189,463
RUN101	8	6763,187	6876,236	626,345	636,814	1372,791	1385,848
RUN102	10	8497,208	9188,18	786,934	850,925	1266,49	1354,558
RUN103	9	11860,198	12954,07	1098,383	1199,688	1052,05	1071,014
RUN104	10	1957,067	2050,139	181,246	189,865	2398,98	2452,002

RUN105	10	6725,972	7289,926	622,898	675,126	1384,438	1397,936
RUN106	9	4527,995	5147,509	419,342	476,715	1632,348	1786,393
RUN107	10	1417,512	1609,207	131,277	149,03	2784,066	2939,938
RUN108	8	7616,131	7932,24	705,337	734,612	1284,759	1306,93
RUN108-V7	6	6832,492	9477,556	632,763	877,725	1352,411	1609,14
RUN109	10	6901,508	7273,511	639,155	673,606	1352,115	1423,194
RUN109-V8	10	10148,381	18990,627	939,851	1758,739	1212,455	1638,572
RUN 110	9	9328,446	13002,999	863,916	1204,219	1176,699	1248,932
RUN 111	10	6511,264	7325,203	603,014	678,393	1404,025	1457,389
RUN112	9	7048,564	7478,999	652,774	692,637	1306,986	1360,74
RUN113	9	12356,053	13808,887	144,305	1278,853	1034,557	1092,529
RUN114	9	7684,015	7990,524	711,623	740,01	1253,039	1271,933
RUN115	10	13787,461	19893,822	1276,869	1842,385	1004,486	1076,055
RUN116	7	7436,527	7863,202	688,702	728,218	1290,734	1318,591
RUN117	10	8693,342	9153,902	805,098	847,751	1178,037	1199,957
RUN118-D2-1	10	7682,515	8340,173	711,485	772,391	1243,669	1285,912
RUN118-D2-2	9	8234,864	9182,68	762,638	850,416	1208,189	1253,689
RUN120-D2-1	7	7624,82	7829,938	706,141	725,137	1256,879	1275,547
RUN120-D2-2	9	8212,925	8423,588	760,606	780,116	1222,98	1229,766
RUN120-Ti-1	8	3996,094	4260,909	370,082	394,607	1738,442	1789,744
RUN120-Ti-2	6	4576,112	5521,62	423,798	511,362	1637,814	1752,188
RUN122-D2-1	10	5698,024	5793,638	527,699	536,554	1508,785	1519,85
RUN122-D2-2	9	5427,878	5571,374	502,681	515,97	1578,241	1597,858
RUN123-D2	8	8112,652	8431,815	751,32	780,878	1220,069	1252,076

Hardness measurement results at 1mN

1mN							
	MPa			***Vickers***		***hm(nm)***	
	#I	***Mean***	***Max***	***Mean***	***Max***	***Mean***	***Max***
RUN1							
RUN2							
RUN3							
RUN4							
RUN5							
RUN6	10	2002.520	2117.273	185.455	196.082	135.714	145.633
RUN7							
RUN8	7	1450.693	1536.279	134.350	142.276	155.450	169.292
RUN9							
RUN10							
RUN11							

RUN12	10	6214.917	8569.439	575.569	793.623	82.867	113.326
RUN13							
RUN14							
RUN15							
RUN16	8	4410.038	12005.395	408.417	1111.830	154.555	289.909
RUN17							
RUN18	10	4734.620	26669.914	438.477	2469.914	120.862	172.004
RUN19	7	5520.155	6079.503	511.226	563.028	80.676	82.724
RUN20							
RUN21	8	8766.126	12609.940	811.839	1167.818	65.581	74.859
RUN22							
RUN23	10	613.030	980.866	56.773	90.839	266.287	419.960
RUN24	9	4637.691	6783.409	429.501	628.217	96.993	157.943
RUN25	10	13886.999	57141.680	1286.087	5291.941	57.193	85.719
RUN26	10	12746.571	26095.912	1180.471	2416.766	60.487	92.327
RUN27							
RUN28	10	1840.584	3727.622	170.458	345.218	154.165	257.247
RUN29	10	825.908	1881.240	76.488	174.223	220.017	259.440
RUN30							
RUN31	10	3912.033	4831.612	362.297	447.460	99.786	129.931
RUN32	10	6208.825	17808.623	575.005	1649.272	89.969	165.616
RUN33	10	4092.443	4961.313	379.005	459.472	96.090	130.114
RUN34	10	17298.693	27583.805	1602.047	2554.561	52.510	116.748
RUN35_D2	10	18394.283	30755.908	1703.789	2848.332	46.145	56.875
RUN35_TINKAP	9	24423.018	34342.945	2261.837	3180.531	38.807	46.816

RUN36							
RUN37							
RUN38	10	16640.777	28366.352	1537.783	2627.033	47.893	58.344
RUN39	9	10806.667	48564.207	1000.815	4497.574	82.975	117.795
RUN40	9	18758.865	25860.791	1737.275	2394.990	42.744	51.606
RUN41	9	23156.971	39746.262	2144.588	3680.937	43.766	78.897
RUN42	10	12739.168	26615.916	1179.786	2466.923	213.019	1.643.712
RUN43	10	17747.838	30864.771	1643.643	2858.414	47.367	56.861
RUN44	10	14822.255	26188.494	1372.702	2425.340	57.992	146.300
RUN45	10	10574.343	29392.818	979.299	2722.095	69.371	133.879
RUN46	10	15573.049	23308.316	1442.234	2158.604	50.679	68.410
RUN47	10	7161.725	15802.866	663.254	1463.517	219.437	800.545
RUN48	9	14593.101	21261.117	1351.480	1969.011	50.309	55.697
RUN49	9	17250.268	28697.721	1597.563	2657.721	49.274	66.617
RUN50	9	14088.014	22268.092	1304.703	2062.268	52.492	79.008
RUN51	10	4519.895	5144.891	418.591	476.473	88.018	102.719
RUN52-D2	9	14714.837	24902.748	1362.754	2306.266	50.438	60.058
RUN52-Ti	10	20992.184	38842.465	1944.105	3597.235	44.809	64.054
RUN53	9	16471.695	27615.418	1525.458	2557.488	48.349	578.824
RUN54	10	13013.586	22713.926	1205.200	2103.557	55.861	98.14
RUN55	9	10621.942	12531.396	983.707	1160.544	56.794	79.465
RUN56	9	9709.637	20636.357	899.218	1911.151	61.923	83.108
RUN57	10	3862.969	4548.127	357.753	421.206	100.612	136.568
RUN58	10	4565.441	5180.791	422.810	479.798	97.590	110.111
RUN59_B	10	18599.121	35382.859	1722.481	3276.838	46.785	62.995

RUN59	10	7378.314	16209.094	683.312	1501.138	69.732	80.875
RUN60_B	7	3794.884	7808.834	351.448	723.183	64.119	96.413
RUN60	9	4286.672	7926.067	396.993	7039.040	64.428	88.884
RUN61	10	8193.029	10219.238	758.764	946.413	63.875	75.035
RUN62	10	4236.905	5839.778	447.950	540.827	88.826	105.140
RUN63	10	1957.595	2140.128	181.295	198.199	130.892	150.909
RUN64	4	1210.636	1253.820	112.118	116.117	165.343	170.009
RUN65	10	17406.848	26208.572	1612.063	2427.199	45.626	52.664
RUN66	7	15588.181	19163.686	1443.635	1774.766	49.040	52.476
RUN67_Bartın1	10	3043.434	3510.667	281855	325.126	110.308	131.822
RUN68_Bartın2	10	9088.701	12927.093	841.713	1197.189	59.716	72.651
RUN69_Bartın3	10	11907.639	16088.892	1102.777	1490.006	56.737	77.614
RUN70	7	2944.150	3051.736	272.660	282.624	109.245	113.396
RUN71	9	10875.601	15128.458	1007.199	1401.060	54.917	62.213
RUN72	8	15205.086	18769.049	1408.156	1738.218	48.327	53.345
RUN73	10	1266.064	1382.163	117.251	128.003	160.376	171.402
RUN74							
RUN75							
RUN76	9	1223.958	1399.515	113.352	129.610	160.427	182.626
RUN77	8	1199.330	1303.516	111.071	120.720	167.370	175.219
RUN78	10	837.641	927.870	77.575	85.931	201.163	218.015
RUN79	9	1017.454	1179.743	94.227	109.257	184.806	199.003
RUN80							
RUN81							
RUN82							

RUN83							
RUN84							
RUN85	6	1712.028	1925.615	158.552	178.333	146.752	163.381
RUN86	9	3180.358	3569.416	294.536	330.567	120.145	127.917
RUN87	9	3229.665	4030.806	299.102	373.297	122.956	136.080
RUN88	10	335.694	960.427	31.089	88.946	632.431	2070.975
RUN89-Ti	7	2725,193	3005,860	252,383	278,375	107,620	113,509
RUN89-D2-1	8	5893,74	6754,879	545,825	625,575	89,582	94,491
RUN89-D2-2	6	9734,786	10582,821	901,547	980,084	65,256	66,907
RUN89-D2-3	4	1204,056	2609,011	111,509	241,623	228,354	363,83
RUN90-D2	8	3938.716	4403.052	364.768	407.771	115.912	120.138
RUN90-V1	8	1355.311	1398.708	125.517	129.536	153.557	156.319
RUN91-D2	10	14422.909	16949.777	1335.719	1569.734	49.129	53.209
RUN91-V2	6	15640.577	17489.959	1448.488	1619.760	47.245	51.044
RUN92	10	4376,255	4839,813	405,289	448,219	107,72	116,305
RUN93-D2	10	4005,348	4492,299	370,939	416,036	1,001	1,004
RUN93-V3	9	3487,987	3854,642	323,026	356,982	104,915	112,23
RUN95	7	18327,260	23704,002	1697,304	2195,249	44,717	53,353
RUN96	8	4446,11	5769,65	411,759	534,333	108,889	122,655
RUN97	6	4456,85	5421,85	412,753	502,122	109,026	115,656
RUN98-D2	9	4022,54	4577,34	372,531	423,911	107,703	118,084
RUN98-V4	9	4131,35	4710,38	382,608	436,232	108,828	118,528
RUN99-D2	10	3507,69	3861,76	324,851	357,641	105,935	110,708
RUN99-V5	8	2167,28	2348,45	200,713	217,492	132,048	139,559
RUN100	8	4483,93	5294,77	415,261	490,354	92,984	101,342

RUN100-V6	8	4251,72	4534,81	393,756	419,972	92,099	94,954
RUN101	10	4155,12	4623,72	384,809	428,207	112,032	116,963
RUN102	10	4847,83	6348,85	448,962	587,972	105,128	113,798
RUN103	10	18558,5	33534,7	1718,72	3105,68	44,063	54,993
RUN104	4	601,786	684,004	55,732	63,346	242,474	259,573
RUN105	8	4826,57	5550,96	446,993	514,079	101,208	107,351
RUN106	4	863,85	1043,23	80,002	96,615	196,999	229,529
RUN107	6	346,588	458,812	32,092	42,491	323,124	381,15
RUN108	7	5912,12	6776,56	547,527	627,583	89,479	97,69
RUN108-V7	9	6042,72	9197,4	559,621	851,779	87,87	118,211
RUN109	10	4601,82	5367,66	426,179	497,103	108,799	116,402
RUN109-V8	5	3573,89	3970,22	330,981	367,685	115,592	120,248
RUN 110	8	3970,22	5459,28	449,833	505,589	85,418	95,432
RUN 111	10	4059,78	4715,63	375,98	436,719	112,512	126,087
RUN112	9	4845,06	5326,6	448,705	493,301	87,871	96,314
RUN113	10	17132,2	23244,2	1586,63	2152,67	44,668	50,131
RUN114	10	2951,09	3348,32	273,303	310,09	104,29	115,13
RUN115	7	17120,1	20222,6	1585,51	1872,83	44,535	49,21
RUN116	4	4066,61	4457,57	376,613	412,819	92,875	97,162
RUN117	7	6384,63	8037,92	591,286	744,398	69,871	73,333
RUN118-D2-1	7	5779,3	6207,17	535,226	574,852	72,384	74,231
RUN118-D2-2	5	6291,92	6664,11	582,7	617,169	70,17	73,321
RUN120-D2-1	10	2572,07	2691,31	238,201	249,245	113,852	119,578
RUN120-D2-2	6	3087,8	3281,8	285,964	303,93	104,639	109,122
RUN120-Ti-1	6	3049,01	3255,33	282,372	301,479	107,786	110,164

RUN120-Ti-2	8	3648,32	3914,98	337,874	362,57	99,055	102,421
RUN122-D2-1	7	2083,88	2390,89	192,99	221,423	134,32	153,751
RUN122-D2-2	3	2565,04	2818,98	237,55	261,069	124,89	128,213
RUN123-D2	9	9899,15	11714,1	916,769	1084,86	57,759	61,549

APPENDIX IV

THICKNESS MEASUREMENTS

RUN	nm	RUN	nm	RUN	nm
RUN 1	38	RUN 42	0	RUN89-D2-1	650
RUN 2	46	RUN 43	90	RUN89-D2-2	900
RUN 3	25	RUN 44	0	RUN89-D2-3	33
RUN 4	35	RUN 45	126	RUN89-Ti	
RUN 5	0	RUN 46	118	RUN 90	320
RUN 6	45	RUN 47	74	RUN 91	67
RUN 7	81	RUN 48	103	RUN 92	1663
RUN 8	304	RUN 49	93	RUN 93	1864
RUN 9	358	RUN 50	134	RUN 95	
RUN 10	114	RUN 51	62	RUN 96	3452
RUN 11	305	RUN 52	51	RUN 97	3990
RUN 12	264	RUN 53	102	RUN 98	658
RUN 13	266	RUN 54	71	RUN 99	755
RUN 14	246	RUN 55	83	RUN 100	304
RUN 15	1092	RUN 56	27	RUN 101	1327
RUN 16	64	RUN 57	157	RUN 102	3360
RUN 17	829	RUN 58	3102	RUN 103	93
RUN 18	81	RUN 59	72	RUN 104	2101
RUN 19	80	RUN 60	47	RUN 105	1643
RUN 20	877	RUN 61	32	RUN 106	2428
RUN 21	69	RUN 62	175	RUN 107	0
RUN 22	120	RUN 63	27	RUN 108	698
RUN 23	117	RUN 64	24	RUN 109	993
RUN 24	1067	RUN 65	59	RUN 110	208
RUN 25	78	RUN 66	56	RUN 111	1372
RUN 26	70	RUN 67	33	RUN112	300
RUN 27	24	RUN 68	41	RUN113	36
RUN 28	57	RUN 69	68	RUN114	309
RUN 29	23	RUN 70	49	RUN115	20
RUN 30 P	98	RUN 71	71	RUN116	309
RUN 31	825	RUN 72	66	RUN117	158

RUN 33	30	RUN 73	72	RUN118-D2-1	137
RUN 34	56	RUN 76	284	RUN118-D2-2	155
RUN 35	317	RUN 77	580	RUN120-D2-1	474
RUN 36	70	RUN 78	866	RUN120-D2-2	421
RUN 37	30	RUN 79	1431	RUN120-Ti-1	1046
RUN 38	85	RUN 85	466	RUN120-Ti-2	548
RUN 39	148	RUN 86	827	RUN122-D2-1	2995
RUN 40	0	RUN 87	603	RUN122-D2-2	4036
RUN 41	0	RUN 88	655	RUN123-D2	45

APPENDIX V

SCRATCH TEST RESULTS

	Fn(N)	*Ft(N)*	*Start F of Scratch*	*Start F of Cracks*	*µm (Max)*	*AE (max)*	*AE (min)*	*Pd (µm)*	*Rd(µm)*
RUN1	0.5-150				0.216	93.38		20.49	10.59
RUN2	0.5-150		26.35		0.235	0.35		19.55	10.33
RUN3	0.5-150		8.86		0.260	4.31		18.12	6.57
RUN4	0.5-150				0.224	6.31		12.88	1.73
RUN5	0.5-150		67.74		0.232	0.5		21.45	7.41
RUN6	0.5-150		37.23		0.223	7.02		20.41	10.53
RUN7	0.5-150		34.89		0.215	9.54		20.95	9.93
RUN8	0.5-150	30.88	52.2		0.206	13.20		23.38	10.37
	1	0.05			0.052	21.81		0.1	0.05
RUN9	0.5-150	30.45	28.86	65.78	0.212	16.26		25.06	10.06
	1.03	0.09			0.087	22.67		0.09	0.02
RUN10	0.5-150	27.75	58.43		0.190	14.62		32.80	9.16
	1	0.07			0.08	8.22		0.24	0.09
RUN11	0.5-150	32.07	28.9		0.214	7.98		23.95	8.94
	1.02	0.02			0.038	6.58		0.19	0.04
RUN12	0.5-150	48.08	0.65		0.335	96.41	3.68	20.33	12.92
	1	0.01			0.14	14.54		0.2	0.07
RUN13	0.5-150	40.51	2.05		0.274	100	36.82	24.69	11.13
	1	0.04			0.034	14.86		0.24	0.03
RUN14	0.5-150	77.98	10.39		0.537	94.99	1.85	25.68	12.43

	1	0.01			0.015	11.39		0.19	0.06
RUN15	0.5-150	82.13	20.71		0.564	86.99	4.22	25.19	16.46
	1.02	0.05			0.053	1.07		0.25	0.16
RUN16	0.5-150	2.59			0.018	72.43		533.93	2.07
	30	2.45			0.082	56.3		5.60	2.94
	50	6.38			6.127	88.06		9.70	5.8
RUN17	0.5-150	78.67		127.42	0.536	86.7	4.54	25.77	10.77
	50	2.36			0.047	53.6		545.62	2.70
	30	2.81			0.094	43.46		5.81	2.82
RUN18	0.5-150	71.78	4.94		0.5	96.34		24.2	16.52
	1	0.02			0.019	0.12		0.222	0.04
RUN19	0.5-200	98.64	25.41		0.5	95.93	2.47	29.41	16.25
	1	0.03			0.028	4.28		0.15	0.02
RUN20	0.5-150	82.52	22.05		0.573	83.14	3.55	25.17	14.92
	1	0.04			0.036	5.76		0.18	0.03
RUN21	0.5-150	80.49	29.84		0.351	56.6	4.78	25.08	9.96
	1	0.03			0.025	0.47		0.17	0.01
RUN22	0.5-150	55.82			0.38	95.37	3.43	23.76	13.13
	1	0.03			0.028	9.14		0.1	0.09
RUN23	0.5-150	43.08		55.89	0.301	96.16	6.13	25.13	11.11
	35	2.97			0.085	74.82		6.61	3.37
	50	6.39			0.116	89.99		10.41	5.77
RUN24	0.5-150	78.08	26.94		0.546	0.17		25.7	15.75
	55	6.69			0.122	91.18		9.65	5.61
RUN25	0.5-150	50.14	4.18	51.40	0.348	100	17.72	25.46	14.60
RUN26	0.5-150	58.72	5.34		0.412	96.06	7.61	22.46	14.37
RUN27	0.5-150	35.36	2.99	53.36	0.245	100	37.69	19.35	11.18
RUN28	0.5-150	71.63	28.59	45.41	0.492	10.29	0.55	18.99	13.20
RUN29	0.5-	68.35	26.71	44.80	0.473	2.74	0.45	23.60	16.39

	150								
RUN30	resputter								
RUN31	0.5-150	69.06	53.77	69.11	0.472	8.06	0.26	20.80	11.91
RUN32	0.5-150	71.66	20.13	40.70	0.493	7.14	0.37	26.82	14.12
RUN33	0.5-150	67.50	50.08	59.21	0.466	8.14	0.30	26.80	12.51
RUN34	0.5-150	74.37	6.50	108.79	0.510	4.27	0.40	21.80	17.41
RUN35-D2	0.5-150	62.06	5.15	121.75	0.427	14.19	0.79	23.20	15.90
RUN35-D2_TiNKap	0.5-150	72.40	36.05	61.54	0.498	1.49	0.31	29.55	17.64
RUN36	resputter								
RUN37	resputter								
RUN38	0.5-150	60.50	6.31	116.35	0.419	6.51	0.76	22.14	15.83
RUN39	0.5-150	48.00	3.04	70.09	0.330	15.81	0.61	23.21	14.56
RUN40	0.5-150	53.22	3.81	138.86	0.365	12.41	0.42	19.87	13.45
RUN41	0.5-150	41.19	2.59		0.282	13.54	0.75	25.58	12.48
RUN42	0.5-150	60.44	4.37	114.39	0.417	7.24	0.64	24.28	15.52
RUN43	0.5-150	33.36	8.83	120.8	0.276	10.61	0.65	14.43	9.74
RUN44	0.5-150	48.66	2.97		0.333	8.02	0.29	21.51	12.32
RUN45	0.5-150	64.05	6.53	88.38	0.440	9.12	0.28	26.70	14.72
RUN46	0.5-150	54.84	20.71	135.37	0.374	11.15	0.29	24.81	14.64
RUN47	0.5-150	52.09	7.31	117.9	0.358	5.02	0.29	16.26	12.36
RUN48	0.5-150	66.75	9.43	114.99	0.46	4.31	0.27	17.26	17.00
RUN49	0.5-150	58.81	61.91	74.55	0.402	0.29	0.25	14.41	11.62
RUN50	0.5-150	58.30	63.86	87.02	0.399	0.18	0.12	19.70	12.06
RUN51	0.5-150	58.69	1.61	24.19	0.403	60.91	0.92	19.06	13.53

RUN52-D2	0.5-150	54.50	62.51	89.31	0.371	0.16	0.12	17.81	10.84
RUN52-Ti	0.5-150	55.29	67.56	104.47	0.379	1.76	0.12	19.80	11.97
RUN53	0.5-150	52.66	41.51	78.82	0.360	10.77	0.22	21.14	10.78
RUN54	0.5-150	53.28	68.52	109.53	0.381	0.17	0.12	21.48	9.80
RUN55	0.5-150	82.18	25.94	91.66	0.569	0.21	0.13	19.52	15.63
RUN56	0.5-150	63.19	48.67	76.68	0.435	3.52	0.13	21.13	12.49
RUN57	0.5-150	72.47	24.98	37.22	0.499	5.05	0.12	22.16	14.44
RUN58	0.5-150	61.81	50.06	56.08	0.430	22.59	0.12	22.18	13.62
RUN59	0.5-150	57.52	65.59		0.397	7.18	0.22	19.10	7.38
RUN60	0.5-150	75.93	32.20	103.52	0.481	16.63	0.13	19.62	13.10
RUN61	0.5-150	81.36	15.64	108.95	0.560	11.54	0.13	17.70	12.09
RUN62	0.5-150	57.71	0.35	21.49	0.398	47.52	2.43	40.20	9.65
RUN63	0.5-150	59.42	0.79	98.05	0.406	67.11	3.66	20.60	11.84
RUN64	0.5-150	56.52	2.61	34.12	0.396	32.14	3.56	17.32	13.69
RUN65	0.5-150	61.38	43.06	89.52	0.402	0.18	0.12	18.33	10.06
RUN66	0.5-150	57.58	56.28	112.24	0.399	0.19	0.12	17.26	12.72
RUN67	0.5-150	52.75	2.48	10.24	0.362	67.89	10.28	24.53	11.68
RUN68	0.5-150	59.77	18.96		0.410	12.53	0.26	21.54	13.90
RUN69	0.5-150	59.22	41.88	101.97	0.406	4.96	0.22	19.15	11.70
RUN70	1-150	62.49	5.42	17.46	0.431	76.78	3.48	24.33	13.26
RUN71	1-150	67.59	0.9	58.92	0.465	96.20	0.53	20.39	13.09
RUN72	1-150	54.14	43.44	71.48	0.373	1.56	0.14	23.65	10
RUN73	1-150	53.35	1.17	33.12	0.370	45.45	4.08	10.66	10.52
RUN74	1-150								
RUN75	1-150								

RUN76	1-150	55.36	2.97	21.82	0.384	98.93	7.65	22.15	11.01
RUN77	1-150	47.11	2.82	10.11	0.325	98.35	10.82	22.91	7.05
RUN78	1-150	46.48	5.83	11.26	0.322	100	2.86	27.37	8.73
RUN79	1-150	57.72	5.64	10.68	0.397	100	0.42	30.29	11.85
RUN80	Long term experiments for rings								
RUN81									
RUN82									
RUN83									
RUN84									
RUN85	1-150	79.37	13.59	31.20	0.471	100	2.27	23.19	16.79
RUN86	1-150	55.97	2.90	22.89	0.434	100	3.98	34.22	10.83
RUN87	1-150	65.64	17.45	37.79	0.456	99.59	5.81	32.24	13.42
RUN88	1-150	77.43	10.49	31.59	0.536	100	0.46	26.40	13.50
RUN89_1	1-150	56.18	16.30		0.386	96.41	0.26	21.90	9.34
RUN89_2	1-150	56.64	51.36		0.389	91.85	0.15	26.05	6.62
RUN89_3	1-150	59.94	32.52		0.381	98.02	0.22	30.10	7.36
RUN89-Ti	1-150	78,16	11,65	70-100	0,525	0.12	0.15	43,87	5,49
RUN90	1-150	63.02	41.68	58.34	0.435	96.29	0.15	24.32	11.07
RUN91	1-150	61.59	50.19	85.07	0.423	3.00	0.12	25.13	12.01
RUN92	1-150	57.37	36.85	49.06	0.398	90.60	0.16	28.75	7.67
RUN93	1-150	74.38	21.98	29.92	0.518	100	0.20	26.33	15.91
RUN95	1-150	48.77	10.35	133.78	0.339	10.13	0.21	24.72	2.99
RUN96	1-150	79.5	13.54	19.8	0.555	48.69	0.41	24.22	1.43
RUN97	1-150	79.67	16.75	35.28	0.485	91.84	0.35	24.72	13.99
RUN98	1-150	65.92	48.84	52.89	0.436	95.03	0.15	26.95	16.27
RUN99	1-150	50.95	5.65		0.364	100	3.57	23.00	8.96
RUN100	1-150	43.89	2.76	22.23	0.310	100	0.30	23.21	5.69
RUN101	1-150	60.85	24.61	51.94	0.449	100	0.14	26.02	12.79
RUN102	1-150	55.58	19.79	58.32	0.370	100	0.36	31.97	0.25
RUN103	1-150	58.58	41.76	72.11	0.392	2.15	0.28	28.31	12.75
RUN104	1-150	51.06	37.23	41.46	0.341	100	1.21	36.14	0.48
RUN105	1-150	53.82	30.28	37.52	0.359	101.13	0.23	23.74	7.55
RUN106	1-150	50.66	24.01	61.19	0.337	100	0.34	22.99	5.71
RUN107	1-150	51,41	4,63	10,31	0,343	100	13,2	29,06	0,17
RUN108	1-150	53,79	44	87	0,435	95,3	1,08	34,29	7,37
RUN109	1-150	55,38	56,2	56,2	0,479	90,5	0,28	28,96	7,53
RUN110	1-150	54,9	30	60	0,365	99,4	0,24	26,91	7,83
RUN111	1-150	68,63	40	45	0,536	95,91	0,27	23,83	12,17
RUN112	1-150	67	31	40	0,459	99,75	0,17	25,63	13,79
RUN113	1-150	65	24-30	50	0,56	16,03	0,14	22,84	13,2
RUN114	1-150	35,68	2-3	20	0,269	100	0,13	23,03	2,48

RUN115	1-150	62,94	20	Slight cracks	0,495	95,73	0,15	22,26	11,42
RUN116	1-150	38,25	2,46	Slight cracks	0,27	100	0,13	36,21	4,58
RUN117	1-150	39,57	2,54	33,14	0,283	96,12	0,13	29,09	4,18
RUN118-1	1-150	47,85	1,18		0,364	97,17	0,29	32,78	6,67
RUN118-2	1-150	38,76			0,285	100	0,4	25,23	3,91
RUN120-1	1-150	45,83	2		0,36	100	0,7	19,09	8,16
RUN120-2	0,5-150	35,06	2,6		0,257	100	0,46	24,18	3,36
RUN120-Ti-1	0,5-150	57,72	13,12	115,16	0,406		0,14	32,08	5,98
RUN120-Ti-2	0,5-150	58,17	36	55	0,548		0,12	30,63	6,92
RUN122-1	0,5-150	62,93	59	59	0,624	7,51	0,14	25,76	15,22
RUN122-2	0,5-150	59,76	12,74	23,23	0,494	99,43	0,14	29,39	9,49
RUN123	0,5-150	64,52	25,94		0,537	30,36	0,13	20,86	12,34

APPENDIX VI

TRIBOMETER TEST RESULTS

	Start(μ)	Time Scale(s)	Distance Scale(m)	Min	Max	Mean	St. Dev.
RUN1	0.345	30	1.4	0.319	0.953	0.859	0.088
RUN2	0.132	384	12.6	0.123	0.881	0.697	0.110
RUN3	0.112	230	7.6	0.108	0.785	0.710	0.081
RUN4	0.127	155	5.05	0.127	0.708	0.658	0.064
RUN5	0.148	130	4.24	0.133	0.740	0.689	0.075
RUN6	0.191	90	2.9	0.142	0.793	0.766	0.054
RUN7	0.156	1.01.E03	33.1	0.110	0.774	0.617	0.197
RUN8	0.446	10	0.33	0.446	0.757	0.717	0.024
RUN9	0.189	205	6.68	0.165	1	0.874	0.111
RUN10	0.289	210	6.85	0.264	0.842	0.734	0.093
RUN11	0.153	60	1.96	0.146	1.087	0.861	0.068
RUN12	0.137	149	4.89	0.122	1.034	0.843	0.115
RUN13	0.145	139	4.57	0.142	0.900	0.819	0.071
RUN14	0.614	44.8	1.47	0.134	1.032	0.829	0.044
RUN15	0.420	24.9	0.82	0.420	1.033	0.854	0.073
RUN16	0.551	190	6.02	0.443	0.858	0.747	0.036
RUN17	0.380	408	13.4	0.019	0.871	0.664	0.071
RUN18	0.576	202	6.62	0.394	0.915	0.801	0.038
RUN19	0.230	140	4.5	0.230	1.085	0.868	0.043
RUN20	0.196	34.8	1.14	0.152	1.060	0.867	0.070
RUN21	0.164	10.5	3.34	0.164	1.014	0.878	0.038
RUN22	0.759	40.9	1.34	0.427	0.904	0.809	0.076
RUN23	0.520	403	13.2	0.412	0.965	0.837	0.054
RUN24	0.145	1510.42	49.53	0.130	0.956	0.777	0.082
RUN25	0.157	3034.70	99.55	0.157	0.952	0.784	0.101
RUN26	0.164	119.23	3.92	0.14	0.908	0.737	0.088
RUN27	0.589	124.20	4.08	0.450	0.715	0.657	0.031
RUN28	0.407	1525.19	50.01	0.407	0.958	0.857	0.088
RUN29	0.158	208.68	6.81	0.158	0.827	0.772	0.043
RUN30	*resputter*						
RUN31	0.110	3616.41	118.62	0.104	0.875	0.344	0.205
RUN32	0.551	480.90	15.77	0.402	0.803	0.773	0.039
RUN33	0.086	253.37	8.29	0.086	0.699	0.619	0.065

RUN34	0.182	2419.16	79.36	0.169	0.940	0.866	0.086
RUN35-D2	0.324	367.69	12.06	0.295	0.943	0.881	0.064
RUN35-D2-TiNKap	0.135	571.28	18.76	0.122	0.819	0.665	0.154
RUN36	*resputter*						
RUN37							
RUN38	0.254	531.73	17.44	0.22	0.936	0.862	0.077
RUN39	0.309	859.34	28.18	0.254	1014	0.914	0.083
RUN40	0.339	283.18	11.30	0.327	0.950	0.891	0.042
RUN41	0.328	353.82	11.62	0.328	1.040	0.989	0.069
RUN42	0.358			0.336	1.013	0.910	0.049
RUN43	0.196	125.72	4.12	0.171	0.986	0.846	0.154
RUN44	0.274	288.17	9.46	0.274	0.925	0.884	0.049
RUN45	0.243	715.36	23.47	0.243	0.959	0.901	0.056
RUN46	0.337	582.53	19.10	0.313	0.902	0.842	0.044
RUN47	0.243	481.91	15.80	0.216	0.889	0.753	0.073
RUN48	0.230	149.08	4.90	0.230	0.859	0.686	0.052
RUN49	0.205	168.97	5.53	0.186	0.851	0.717	0.043
RUN50	0.248	173.95	5.72	0.197	0.871	0.730	0.070
RUN51	0.852	94.45	3.11	0.547	0.987	0.814	0.048
RUN52-D2	0.232	173.95	5.72	0.177	0.882	0.778	0.071
RUN52-Ti	0.226	159.03	5.22	0.217	0.856	0.770	0.097
RUN53	0.180	139.18	4.56	0.175	0.795	0.624	0.055
RUN54	0.362	46.49	1.54	0.362	0.887	0.795	0.044
RUN55	0.525	19.91	0.66	0.5	0.993	0.873	0.092
RUN56	0.105	273.41	8.95	0.105	0.741	0.665	0.072
RUN57	0.273	64.64	2.10	0.273	1.214	0.971	0.141
RUN58	0.420	467.21	15.33	0.225	1.426	1.344	0.102
RUN59	0.134	119.31	3.92	0.134	0.735	0.683	0.046
RUN60	0.165	860.70	28.21	0.159	0.818	0.779	0.046
RUN61	0.140	233.61	7.63	0.133	0.883	0.694	0.091
RUN62	0.617	119.30	3.93	0.279	0.905	0.845	0.028
RUN63	0.552	36.61	1.19	0.535	0.839	0.727	0.027
RUN64	0.112	550.34	18.03	0.112	0.965	0.762	0.052
RUN65	0.182	894.63	29.31	0.167	0.787	0.671	0.054
RUN66	0.470	1078.45	35.37	0.455	0.853	0.698	0.041
RUN67_Bartın1	0.344	114.37	27.89	0.324	0.716	0.642	0.022
RUN68_Bartın2	0.108	198.88	6.53	0.108	0.751	0.648	0.069
RUN69_Bartın3	0.301	69.64	2.29	0.263	0.795	0.600	0.048
RUN70	0.541	29.84	0.97	0.541	0.69	0.844	0.072
RUN71	0.328	909.12	29.81	0.199	0.823	0.691	0.143

RUN72	0.246	471.87	15.49	0.239	0.839	0.765	0.046
RUN73	0.43	4.27	0.13	0.327	0.953	0.843	0.04
RUN76	0.931	149.07	4.90	0.91	1.154	1.09	0.024
RUN77	0.578	99.76	3.23	0.444	0.797	0.745	0.03
RUN78	0.367	114.72	3.71	0.367	0.805	0.716	0.021
RUN79	0.480	209.49	6.85	0.380	0.834	0.740	0.044
RUN80	Long hours ring experiments						
RUN81							
RUN82							
RUN83							
RUN84							
RUN85	0.158	244.53	8.02	0.155	0.821	0.747	0.035
RUN86	0.535	444.10	14.45	0.526	0.886	0.643	0.052
RUN87	0.561	2276.19	74.27	0.156	1.516	1.183	0.189
RUN88	0.094	2015.955	65.78	0.094	1.675	1.139	0.196
RUN89-D2-2	0.250	565.66	18.54	0.210	0.850	0.777	0.107
RUN89-D2-3	0.226	384.07	12.57	0.226	1052	0.929	0.097
RUN91	0.413	29.86	0.94	0.333	0.697	0.682	0.016
RUN92	0.583	486.96	15.96	0.583	0.900	0.829	0.046
RUN93	0.210	19.31	0.66	0.210	0.856	0.780	0.044
RUN95	0.249	19.99	0.63	0.249	0.707	0.612	0.043
RUN96	0.741	149.7	4.84	0.525	1.231	0.997	0.119
RUN97	0.828	64.67	2.11	0.659	1.116	0.865	0.099
RUN98	0.702	19.92	0.66	0.665	0.957	0.913	0.018
RUN99	0.708	49.92	1.63	0.533	1095	0.907	0.081
RUN100	0.813	19.98	0.62	0.582	0.956	0.847	0.043
RUN101	0.647	38.28	1.23	0.550	0.827	0.777	0.027
RUN102	0.504	204	6.69	0.41	1.07	0.935	0.061
RUN103	0.381	59.65	1.99	0.357	0.897	0.781	0.044
RUN104	0.1443	26.16	0.84	0.089	0.204	0.137	0.024
RUN105	0.345	2.08	0.04	0.345	0.868	0.814	0.027
RUN106	0.103	67.22	50.93	0.103	1.208	0.882	0.116
RUN107	0.093	1.02	0.04	0.044	0.179	0.077	0.014
RUN108	0.815	114.53	3.74	0.614	0.979	0.858	0.054
RUN109	0.603	41.41	36.01	0.432	0.939	0.863	0.073
RUN110	0.689	9.19	0.28	0.515	0.881	0.789	0.046
RUN111	0.586	67.96	2.26	0.553	1.041	0.919	0.068
RUN112	1.279	1.17	0	0.758	1.399	0.957	0.06
RUN113	0.119	369	12.07	0.119	0.897	0.787	0.092
RUN114	0.587	79.51	2.58	0.587	0.882	0.812	0.05
RUN115	0.312	159.37	5.21	0.132	0.768	0.729	0.073

RUN116	0.584	186.89	6.1	0.308	1.024	0.748	0.096
RUN117	0.608	5.02	0.13	0.509	0.946	0.829	0.043
RUN118-D2-1	0.554	44.9	1.45	0.464	0.829	0.728	0.117
RUN118-D2-2	0.314	36.36	1.19	0.263	0.775	0.707	0.059
RUN120-D2-1	0.153	19.97	0.63	0.153	0.933	0.869	0.04
RUN120-D2-2	0.3	22.45	0.75	0.241	0.87	0.836	0.04
RUN120-Ti-1	0.437	5.09	0.13	0.318	0.943	0.493	0.071
RUN120-Ti-2	0.132	12.19	0.38	0.132	0.654	0.517	0.056
RUN122-D2-1	0.546	3.77	0.13	0.546	1.466	1.109	0.066
RUN122-D2-2	0.679	149.54	4.84	0.487	0.96	0.809	0.048
RUN123-D2	0.78	524.12	17.09	0.175	0.797	0.754	0.102